

1                   **Leaf trait acclimation amplifies simulated climate warming**  
2                   **in response to elevated carbon dioxide.**

3  
4                   **Authors:** Marlies Kovenock<sup>1</sup> and Abigail L.S. Swann<sup>2,1</sup>

5  
6                   <sup>1</sup>Department of Biology, University of Washington, Box 351800, Seattle, WA 98195, USA

7                   <sup>2</sup>Department of Atmospheric Sciences, University of Washington, Box 351640, Seattle, WA  
8                   98195, USA

9  
10                  Corresponding author: Marlies Kovenock (kovenock@uw.edu)

11  
12                  **Key Words:**

13                  global warming, vegetation feedbacks, plant traits, carbon cycle, climate impact

14  
15                  **Key Points:**

- 16                  • Acclimation of leaf traits to elevated CO<sub>2</sub> significantly altered global climate and carbon  
17                  cycling in Earth system model experiments
- 18                  • Higher carbon cost of building leaf area under elevated CO<sub>2</sub> offsets gains in leaf area,  
19                  productivity, and evapotranspiration
- 20                  • Results identify an urgent need to collect observations to constrain uncertainty in plant  
21                  trait responses to a changing climate

22 **Abstract**

23 Vegetation modifies Earth's climate by controlling the fluxes of energy, carbon, and water. Of  
24 critical importance is a better understanding of how vegetation responses to climate change will  
25 feedback on climate. Observations show that plant traits respond to elevated carbon dioxide  
26 concentrations. These plant trait acclimations can alter leaf area and thus productivity and  
27 surface energy fluxes. Yet, the climate impacts of plant structural trait acclimations remain to be  
28 tested and quantified. Here we show that one leaf trait acclimation in response to elevated carbon  
29 dioxide – a one third increase in leaf mass per area – significantly impacts climate and carbon  
30 cycling in Earth system model experiments. Global net primary productivity decreases (-5.8  
31 PgC/yr, 95% confidence interval, CI<sub>95%</sub> -5.5 to -6.0), representing a decreased carbon dioxide  
32 sink of similar magnitude to current annual fossil fuel emissions (8 PgC/yr). Additional  
33 anomalous terrestrial warming (+0.3°C globally, CI<sub>95%</sub> 0.2 to 0.4), especially of the northern  
34 extratropics (+0.4°C, CI<sub>95%</sub> 0.2 to 0.5), results from reduced evapotranspiration and enhanced  
35 absorption of solar radiation at the surface. Leaf trait acclimation drives declines in productivity  
36 and evapotranspiration by reducing leaf area growth in response to elevated carbon dioxide, as a  
37 one third increase in leaf mass per area raises the cost of building leaf area and productivity fails  
38 to fully compensate. Our results suggest that plant trait acclimations, such as changing leaf mass  
39 per area, should be considered in climate projections and provide additional motivation for  
40 ecological and physiological experiments that determine plant responses to environment.

41

42 **Significance Statement**

43 Plants have been observed to change their traits, such as the thickness of leaves, in  
44 response to future environmental conditions, but the implications of these changes for climate

45 have not yet been quantified. We show that changes in plant traits could have large-scale climate  
46 implications, including higher temperatures and relative decreases in plant photosynthesis which  
47 have not been previously accounted for. Our findings suggest an urgent need for observations of  
48 how plant traits will respond to future environmental conditions as well as a need for a better  
49 understanding of the underlying mechanisms so that they can be included in climate projections.

50

## 51 **1 Introduction**

52         Feedbacks between vegetation and climate change are of critical importance to future  
53 climate projections but remain highly uncertain (Arora et al., 2013; Friedlingstein et al., 2014;  
54 Lovenduski & Bonan, 2017; Pu & Dickinson, 2012). Vegetation strongly influences the Earth's  
55 climate by controlling the fluxes of carbon, water, and energy between the land surface and the  
56 atmosphere (Bonan, 2008). Changes in these fluxes can alter biogeochemical warming of the  
57 Earth through atmospheric concentrations of carbon dioxide (CO<sub>2</sub>), and biogeophysical warming  
58 due to Earth surface properties such as evapotranspiration, albedo, and roughness. Since the start  
59 of the industrial era, Earth's vegetation has removed about 30% of anthropogenic CO<sub>2</sub> emissions  
60 from the atmosphere (Ciais et al., 2013). Transpiration, the biologically controlled flux of water  
61 from soil through plants into the atmosphere, makes up an estimated 60% of current terrestrial  
62 water fluxes (Wei et al., 2017), which physically cool the land surface. Rising CO<sub>2</sub>  
63 concentrations are expected to have profound and wide reaching effects on vegetation  
64 functioning and growth, with important implications for global carbon uptake and  
65 evapotranspirative cooling. Yet, large uncertainty exists in the magnitude, and even the sign, of  
66 vegetation feedbacks on climate change (Arora et al., 2013; Friedlingstein et al., 2014;  
67 Lovenduski & Bonan, 2017; Pu & Dickinson, 2012). This uncertainty stems in large part from

68 the challenge of representing complex and diverse life-forms at the global-scale in the Earth  
69 system models used to project future climate (Lovenduski & Bonan, 2017). Key biological  
70 processes must be missing or poorly constrained but we lack a clear understanding of which  
71 processes are essential for predicting climate and carbon cycling changes.

72         Incorporating observations of plant trait distributions and their responses to  
73 environmental drivers into Earth system models is proposed as a way to improve predictions of  
74 ecosystem functioning (Fisher et al., 2015; Kattge & Knorr, 2007; Kattge et al., 2011; Pavlick et  
75 al., 2013; Reich et al., 2014; Reichstein et al., 2014; Scheiter et al., 2013; Van Bodegom et al.,  
76 2012; Verheijen et al., 2015, 2013; Wright et al., 2004). Trait databases and studies that  
77 aggregate observations across species are beginning to make it possible to characterize current  
78 plant trait distributions and their responses to environmental drivers at the global scale (e.g.  
79 Kattge et al., 2011; Kattge & Knorr, 2007; Niinemets, 2001; Van Bodegom et al., 2012;  
80 Verheijen et al., 2013; Wright et al., 2004). However, the biogeographic relationship between  
81 traits and climate across ecosystems, caused primarily by environmental filtering, does not tell us  
82 about short term responses to changes in climate within an ecosystem, caused by acclimation  
83 (Van Bodegom et al., 2012; Verheijen et al., 2013). The climate impacts of these two distinct  
84 responses, environmental filtering and acclimation, have been tested in previous work.

85         Studies focused on environmental filtering have shown that allowing traits to vary  
86 temporally based on observed spatial relationships between these traits and environmental  
87 drivers (i.e. space-for-time substitution) has carbon uptake and climate implications (Verheijen et  
88 al., 2013, 2015). This approach estimates the integrated outcome of numerous biological  
89 responses to climate (e.g. adaptation, changes in species distribution, acclimation) (Van  
90 Bodegom et al., 2012; Verheijen et al., 2015). However, it does not separate the impacts of

91 individual biological responses (e.g. acclimation, adaptation, species turnover) from one another  
92 and therefore cannot mechanistically explain the underlying causes of trait variation (Verheijen  
93 et al., 2013). Further, it is uncertain if space-for-time relationships used in the environmental  
94 filtering approach will hold under future climate in part because acclimation of traits may alter  
95 these trait-environment relationships (Fisher et al., 2015; Verheijen et al., 2015). Acclimation  
96 responses can differ in magnitude and even direction from trait responses to environmental  
97 filtering (e.g. Poorter et al., 2009; Verheijen et al., 2013).

98         Other studies have directly investigated the influence of some trait acclimations to  
99 temperature and elevated CO<sub>2</sub> (e.g. photosynthetic and stomatal conductance rates) and found  
100 profound effects on large-scale climate and carbon cycling (Betts et al., 1997; Cao et al., 2010;  
101 Lombardozzi et al., 2015; Pu & Dickinson, 2012; Sellers et al., 1996; Smith et al., 2017).  
102 Acclimation occurs within the same individual plant and on short time scales (e.g. a growing  
103 season), making it immediately relevant for 21st century climate. Prior studies have focused on  
104 rate traits and have not considered the potential climate feedbacks of plant structural traits. Trait  
105 responses to climate change that alter plant structure could feedback on climate and carbon  
106 cycling by modifying the surface areas (e.g. leaf area) over which the rates of photosynthesis and  
107 stomatal conductance are summed.

108         Among the most widely observed plant structural trait responses to elevated CO<sub>2</sub> is an  
109 increase in leaf mass per area (g leaf carbon / m<sup>2</sup> leaf area). Leaf mass per area represents the  
110 carbon cost of building leaf area and is a quantity commonly used in Earth system models to  
111 convert from carbon available for leaf growth to leaf area. Field and greenhouse manipulation  
112 experiments show that leaf mass per area increases by as much as one third in response to  
113 elevated CO<sub>2</sub> in a wide range of C<sub>3</sub> plants, including trees, shrubs, and crops, across a variety of

114 ecosystems on many continents (Ainsworth & Long, 2005; Medlyn et al., 1999, 2015; Poorter et  
115 al., 2009). Acclimation to warming temperatures could potentially offset leaf mass per area  
116 increases due to elevated CO<sub>2</sub> but is limited to cold regions such as the boreal and arctic (Poorter  
117 et al., 2009). Most Earth system models project increases in leaf area in response to CO<sub>2</sub> over the  
118 21st century (Mahowald et al., 2016; Swann et al., 2016), which are expected to negatively  
119 feedback on climate change by promoting carbon uptake from the atmosphere and  
120 evapotranspirative cooling over land (Betts et al., 1997; Bounoua et al., 2010; Pu & Dickinson,  
121 2012). However, few models capture the decreased sensitivity of leaf area index to increases in  
122 leaf biomass at elevated CO<sub>2</sub> because they fail to represent the concomitant increase in leaf mass  
123 per area (De Kauwe et al., 2014; Medlyn et al., 2015).

124         Here we quantify the potential extent of climate and carbon cycling impacts of leaf mass  
125 per area acclimation to rising CO<sub>2</sub> using a series of Community Earth System Model coupled  
126 atmosphere-land-carbon cycle simulations (Table S1). In the model, vegetation responds to  
127 climate by changing carbon assimilation, stomatal conductance, biomass, and leaf area. These  
128 vegetation responses can induce biogeophysical warming through feedbacks on the surface  
129 energy balance and atmosphere via changes in albedo, evapotranspiration, and surface  
130 roughness. We quantify the additional climate impacts, beyond those of elevated CO<sub>2</sub>, of leaf  
131 mass per area acclimation to CO<sub>2</sub> as the difference between a leaf acclimation experiment and a  
132 climate change control simulation (CCLMA - CC). The level of leaf acclimation, a one third  
133 increase in leaf mass per area in C<sub>3</sub> plants, was estimated from the upper bound of acclimation to  
134 a doubling of CO<sub>2</sub> (355ppm to 710ppm) from Poorter et al. (2009)'s meta-analysis of  
135 approximately 200 studies, which provides the most plant-type-specific CO<sub>2</sub> acclimation  
136 relationships for leaf mass per area currently available. The control simulation (CTRL) provides

137 a reference for whether the effects of leaf acclimation at elevated CO<sub>2</sub> (CCLMA - CC) moderate  
138 (e.g. reduce the increase in leaf area) or enhance (e.g. further increase leaf area) changes due to  
139 elevated CO<sub>2</sub> alone (CC - CTRL). We also estimate the effects of leaf mass per area acclimation  
140 to temperature (TCCLMA - CC) and the historical influence of changing leaf mass per area  
141 (LMA - CTRL). As atmospheric CO<sub>2</sub> concentration is held invariant over time in all simulations,  
142 biogeochemical warming is estimated from the difference in net primary productivity.

143

## 144 **2 Materials and Methods**

145 This study used the Community Earth System Model version 1.3beta11 with interactive  
146 land and biogeochemistry (CLM4.5-BGC; Oleson et al., 2013), atmosphere (CAM5; Neale et al.,  
147 2012), mixed-layer ocean (Neale et al., 2012), and sea ice (CICE4; Hunke & Lipscomb, 2010)  
148 models. Simulations that couple the land and atmosphere, such as performed here, are required to  
149 quantify the climate impacts of changes in the land surface, as they capture the atmospheric  
150 response and land-atmosphere feedbacks. To allow for ocean heat transport and atmosphere-  
151 ocean interaction while retaining computational economy, we used a mixed-layer ocean model  
152 with prescribed lateral heat fluxes rather than a more computationally expensive full dynamical  
153 ocean model. We ran the simulations with a spatial resolution of approximately 1.9° by 2.5°  
154 gridcells. The biogeochemistry model represents a full terrestrial carbon cycle with growth,  
155 mortality, and decay - and hence leaf area and carbon storage in above- and below-ground pools.  
156 The distribution of 16 plant functional types was prescribed by a map of present day vegetation  
157 and held invariable; however, under unsuitable growing conditions, plants diminish to a  
158 minimum leaf area.

159 The climate change control simulation (CC; 2xCO<sub>2</sub>, no leaf acclimation) represents the  
160 mean climate state when atmospheric CO<sub>2</sub> is fixed at 710ppm. The CO<sub>2</sub> leaf acclimation  
161 experiment (CCLMA; 2xCO<sub>2</sub>, +1/3 leaf mass per area) is identical to the climate change control  
162 simulation (CC) except that it includes a plausible extent of leaf mass per area acclimation to  
163 CO<sub>2</sub> in all C<sub>3</sub> plants (Poorter et al., 2009). (See supporting information Text S1.2 for details.) A  
164 second experiment (TCCLMA; 2xCO<sub>2</sub>, no change in leaf mass per area in boreal and arctic  
165 biomes, +1/3 leaf mass per area in all other C<sub>3</sub> plants) tests the impact of leaf acclimation to both  
166 CO<sub>2</sub> and temperature (Poorter et al., 2009). (See supporting information Text S1.3 and S2.1 for  
167 further details.) Leaf mass per area acclimation to CO<sub>2</sub> and temperature were estimated using the  
168 most plant-type-specific acclimation relationships currently available (Poorter et al., 2009). A  
169 third experiment (CCLMAPS; 2xCO<sub>2</sub>, +1/3 leaf mass per area, +1/3 max photosynthetic rates)  
170 quantifies the increase in maximum photosynthetic rates required to offset the biogeophysical  
171 warming due CO<sub>2</sub> acclimation of leaf mass per area. A fourth experiment (LMA; 1xCO<sub>2</sub>, +1/3  
172 leaf mass per area) tests the sensitivity of historical climate to increased leaf mass per area. As  
173 the default model calculates maximum photosynthetic rates ( $V_{\text{cmax}25}$ ,  $J_{\text{max}25}$ ,  $T_{\text{p}25}$ ) from leaf mass  
174 per area, we modified this relationship so that these rates did not differ between the control and  
175 CCLMA, TCCLMA, and LMA experiment simulations. (See supporting information Text S1.2  
176 for details.) This represents a conservative estimate of acclimation of maximum photosynthetic  
177 rates to CO<sub>2</sub>, as evidence supports a decrease in these rates in response to elevated CO<sub>2</sub>  
178 (Ainsworth & Long, 2005; Leakey et al., 2012; Rogers et al., 2017; Smith & Dukes, 2013). All  
179 simulations include temperature acclimation of maximum photosynthetic rates (Kattge & Knorr,  
180 2007; Oleson et al., 2013). All elevated CO<sub>2</sub> simulations (CC, CCLMA, TCCLMA, CCLMAPS)  
181 include the effects of CO<sub>2</sub> radiative forcing, CO<sub>2</sub> fertilization, and gains in water use efficiency.



182 A separate control simulation (CTRL; 1xCO<sub>2</sub>, no leaf acclimation) represents the equilibrium  
183 climate state when CO<sub>2</sub> concentration is fixed at 355ppm, a common baseline for Earth system  
184 model simulations.

185 All simulations were integrated for 85 years, except the CCLMAPS experiment was  
186 integrated for 44 years. All experiment simulations were initiated by branching from the  
187 beginning of year 56 of the control run (CTRL). Temperature, leaf area index, net and gross  
188 primary productivity, evapotranspiration and live carbon pools (leaf, live stem, live root, and fine  
189 root) reached equilibrium before year 30 in each simulation. The first 30 years of each simulation  
190 were discarded to allow for spin up. The remaining years were used in our analysis and represent  
191 many samples of the equilibrium state. (Model results to be made available from University of  
192 Washington library archive at publication.)

193 We use annual mean changes in biogeophysical warming and net primary productivity to  
194 quantify the upper bound of the potential climate and carbon cycling influences of leaf mass per  
195 area acclimation. We tested for differences between simulations in the annual mean at the global,  
196 latitude band, zonal mean (average for a given latitude), and gridcell scales using bootstrap  
197 methods with model years as the unit of replication. Spatial relationships between variables at  
198 the gridcell scale were tested using simple, multiple, and stepwise linear regression methods on  
199 annual mean values. Differences and relationships were considered significant at the 95% level.  
200 (See supporting information Text S1.4 for details.) Latitude bands were defined as southern  
201 extratropics (60°S to 20°S), tropics (20°S to 20°N), northern extratropics (20°N to 65°N), and  
202 northern high latitudes (65°N to 90°N).

203 Biogeochemical warming was calculated by converting the change in net primary  
204 productivity to a change in atmospheric CO<sub>2</sub> level (2 PgC to 1 ppm). After accounting for

205 compensatory carbon uptake by the ocean of 60-85% (Archer et al., 2009; Broecker et al., 1979),  
206 we converted the change in atmospheric CO<sub>2</sub> concentration to a radiative forcing in W/m<sup>2</sup>  
207 following the methods of Hansen et al. (1998) and Myhre et al. (1998). The resulting global  
208 temperature change was then estimated from the forcing using a range of climate sensitivities  
209 (temperature change due to a doubling of CO<sub>2</sub>) from 1.5 to 4.5°C.

210

### 211 **3 Results**

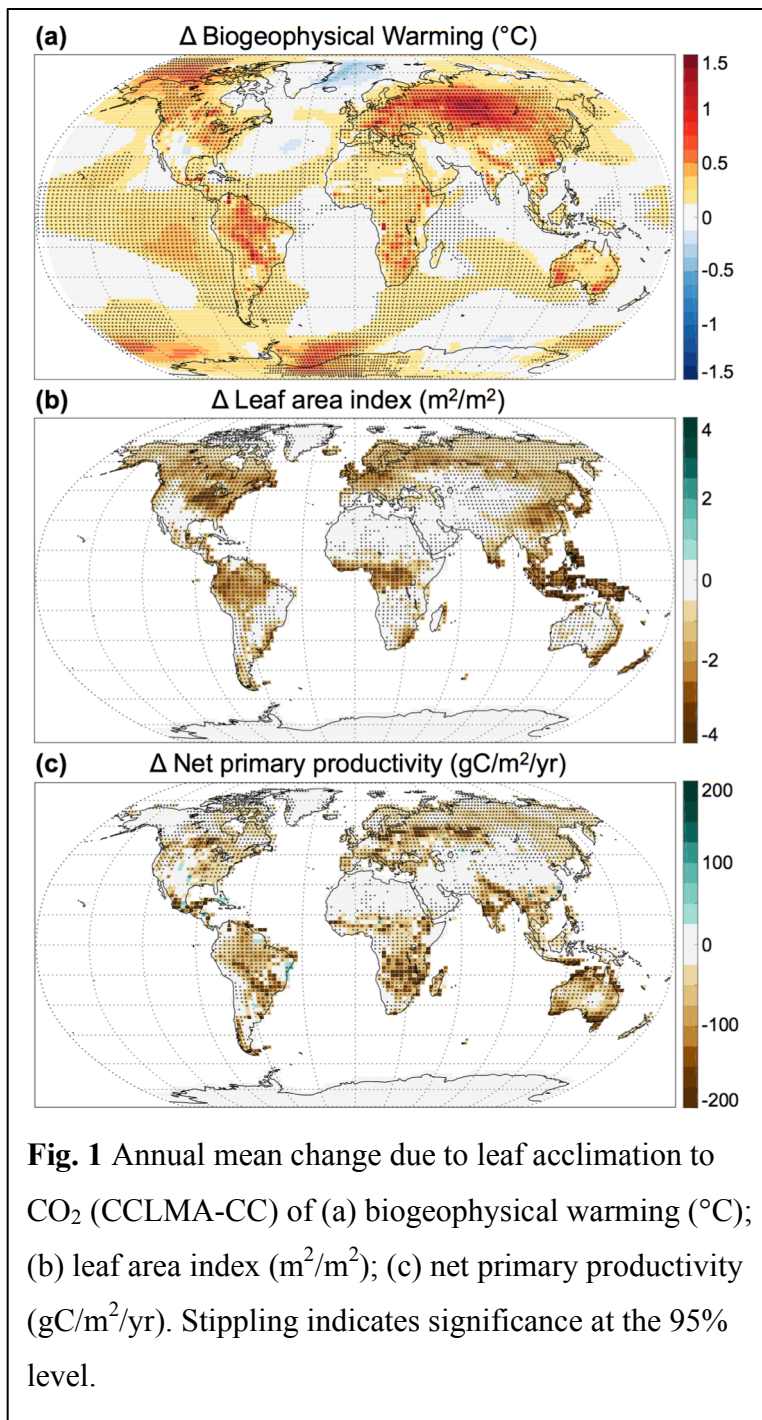
#### 212 **3.1 Biogeophysical Warming**

213 Acclimation of leaf mass per area to elevated CO<sub>2</sub> induced significant biogeophysical  
214 warming in addition to the warming caused by the radiative effects of a doubling of CO<sub>2</sub> in Earth  
215 system model experiments. The change in temperature from the direct effects of a doubling of  
216 CO<sub>2</sub> (from 355ppm to 710ppm) in our model (CC - CTRL) was 5.0°C (CI<sub>95%</sub> 5.0 to 5.1), with a  
217 higher mean warming over land of 6.1°C (CI<sub>95%</sub> 6.0 to 6.1). The influence of doubling CO<sub>2</sub>  
218 included plant responses such as carbon fertilization (Oleson et al., 2013) and increased water  
219 use efficiency (+27% for CC - CTRL, CI<sub>95%</sub> 27 to 28) but did not account for acclimation of leaf  
220 mass per area. Consideration of leaf mass per area acclimation to CO<sub>2</sub> (CCLMA - CC) increased  
221 annual mean temperature over land by an additional +0.3°C (CI<sub>95%</sub> 0.2 to 0.4, Fig. 1a, Table 1,  
222 S2) and +0.2°C (CI<sub>95%</sub> 0.1 to 0.2) globally on top of the direct effects of CO<sub>2</sub>. This acclimation  
223 driven warming was especially pronounced over land in the northern extratropics (+0.4°C, CI<sub>95%</sub>  
224 0.2 to 0.5) due to above average warming over Eurasia (Fig. 1a, Fig. 2a, Table 1). The influence  
225 of temperature acclimation of leaf mass per area (TCCLMA - CC) was limited to cold biomes  
226 and did not significantly alter the amount of additional warming over land and globally due to  
227 CO<sub>2</sub> acclimation (supporting information Text S2.1; Fig. S1). The influence of leaf mass per area

228 changes at historical CO<sub>2</sub> levels  
 229 (LMA - CTRL) was also small  
 230 (supporting information Text  
 231 S2.2).

232 Leaf trait acclimation  
 233 enhanced biogeophysical warming  
 234 over land under future CO<sub>2</sub> levels  
 235 by offsetting the CO<sub>2</sub> induced  
 236 increase in leaf area index (m<sup>2</sup> leaf  
 237 area / m<sup>2</sup> ground; ). Doubling of  
 238 CO<sub>2</sub> (CC - CTRL) increased the  
 239 annual mean leaf area index by 1.2  
 240 m<sup>2</sup>/m<sup>2</sup> (CI<sub>95%</sub> 1.2 to 1.2) in our  
 241 simulations. This magnitude of  
 242 change is at the high end of  
 243 CMIP5 model leaf area responses  
 244 to RCP8.5 over the 21st century  
 245 (Mahowald et al., 2016). Inclusion  
 246 of leaf mass per area acclimation  
 247 strongly limited the increase in

248 leaf area index to 0.3 m<sup>2</sup>/m<sup>2</sup> (CI<sub>95%</sub> 0.2 to 0.3) over the ambient CO<sub>2</sub> simulation (CCLMA -  
 249 CTRL). This attenuation of leaf area growth occurred in almost all vegetated areas (Fig. 1b, Fig.  
 250 2b, Table 1). However, leaf area index decreased more in response to leaf acclimation in places



251 with high initial leaf areas, as shown by the negative spatial relationship ( $R^2 = 0.83$ , Fig. S2a)  
 252 between leaf area index in the control climate change case (CC) and the change in leaf area index  
 253 in response to leaf acclimation (CCLMA - CC).

254 The reduced increase in leaf area in response to leaf trait acclimation (CCLMA - CC)  
 255 induced biogeophysical warming over land by shifting the balance between surface energy  
 256 budget terms. Near surface temperature warmed in response to a moderation of the increase in  
 257 evapotranspirative cooling and an increase in solar radiation absorbed at the Earth's surface (Fig.  
 258 2, Fig. 3c, Table 1, Table S2). These two factors shifted additional energy to sensible heat, the  
 259 term in the surface energy balance that directly drives surface temperature changes. In the  
 260 tropics, warming was primarily the result of reduced evapotranspiration, followed by greater  
 261 solar radiation absorbed at the surface (Fig. 2c,d, Table 1, S2). In the extratropics, increased

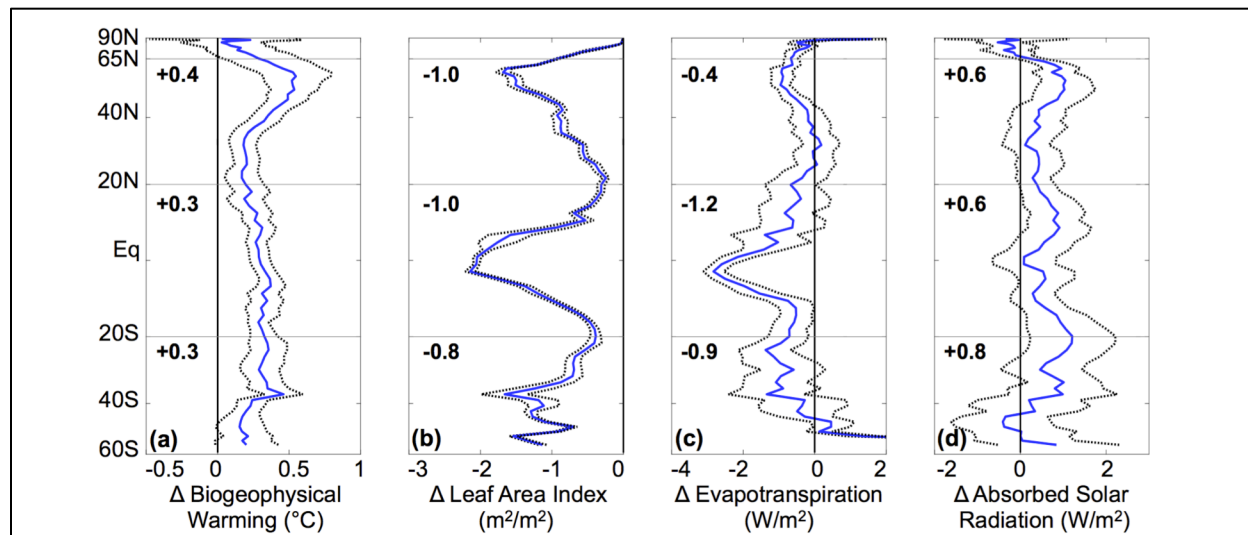


**Fig. 2** Zonal annual mean change over land due to leaf acclimation to CO<sub>2</sub> (CCLMA - CC) of (a) biogeophysical warming (°C); (b) leaf area index (m<sup>2</sup>/m<sup>2</sup>); (c) evapotranspiration (W/m<sup>2</sup>); and (d) net solar radiation absorbed at the surface (W/m<sup>2</sup>). The mean difference is shown in blue, along with the 95% bootstrap confidence interval (dashed black) and average zonal mean change on land (bold numbers) for each latitude band (bounded by dashed lines).

	Global		S. Extratropics		Tropics		N. Extratropics	
Biogeophysical Warming (°C)	0.3	(0.1%)	0.3	(0.1%)	0.3	(0.1%)	0.4	(0.1%)
Net primary productivity (PgC/yr)	-5.8	(-6.4%)	-0.8	(-9.1%)	-2.5	(-6.1%)	-2.1	(-6.2%)
Leaf area index (m <sup>2</sup> /m <sup>2</sup> )	-0.9	(-26.0%)	-0.8	(-24.0%)	-1.0	(-24.3%)	-1.0	(-27.4%)
Evapotranspiration (W/m <sup>2</sup> )	-0.7	(-1.5%)	-0.9	(-1.6%)	-1.2	(-1.6%)	-0.4	(-1.1%)
Transpiration (W/m <sup>2</sup> )	-1.4	(-5.8%)	-1.9	(-7.2%)	-1.7	(-4.6%)	-1.1	(-6.7%)
Leaf Evaporation (W/m <sup>2</sup> )	-0.8	(-8.6%)	-0.7	(-8.5%)	-1.3	(-8.3%)	-0.5	(-9.0%)
Soil Evaporation (W/m <sup>2</sup> )	1.4	(9.5%)	1.6	(7.0%)	1.9	(10.6%)	1.3	(9.9%)
Absorbed Solar Radiation (W/m <sup>2</sup> )	0.6	(0.4%)	0.8	(0.5%)	0.6	(0.4%)	0.6	(0.4%)

Note: All changes significant at the 95% level. Percent change ((CCLMA - CC)/CC) in parentheses. Confidence intervals reported in Table S2.

262 absorption of solar radiation and reduced evapotranspiration induced warming in more equal  
 263 proportion (Fig. 2b,c, Table 1, S2). The strong influence on the surface energy budget of  
 264 evapotranspiration in the tropics and the combination of evapotranspiration and solar radiation in  
 265 the mid-latitudes is consistent with previous studies (Bonan, 2008).

266 Evapotranspiration is the combination of several contributing water fluxes. Reduced  
 267 transpiration (CCLMA - CC) represented the largest contribution to evapotranspiration declines  
 268 in all regions, followed by lower evaporation from leaf surfaces (Table 1, S2). However, greater  
 269 soil evaporation partially offset the decline from transpiration and leaf evaporation. Reductions  
 270 in evapotranspiration were spatially positively related to changes in leaf area (CCLMA - CC;  $R^2$   
 271 = 0.32, Fig. S2b). As leaf area provides the surface area over which transpiration and leaf  
 272 evaporation occur, the acclimation-induced reduction of leaf area index diminished  
 273 evapotranspiration to drive biogeophysical warming.

274 More solar radiation reached land when leaf mass per area acclimation was included (Fig.  
 275 2d, 3c, Table 1) due to reduced low cloud cover over the tropics and northern extratropics (Fig.  
 276 S3a). Acclimation-driven warming decreased the relative humidity of the lower atmosphere in  
 277 these regions (Fig. S3b), making it less likely for water vapor to saturate the air and condense to  
 278 form clouds. Relative humidity decreased because warming of the atmosphere (Fig. S3c) raised  
 279 the saturation vapor pressure, outcompeting the influence of greater absolute amounts of water

280 vapor (i.e. specific humidity) in some areas (Fig. S3d). The overall increase in solar radiation at  
281 the surface demonstrates that the effect of reduced cloud cover overwhelmed the opposing  
282 influence of a small surface albedo increase. Albedo increased because the reduced increase in  
283 leaf area index (CCLMA - CC) allowed more radiation to reach and reflect away from bare  
284 ground which is brighter than vegetation (Bonan, 2008; Oleson et al., 2013). Albedo changes  
285 (Fig. S4) were measured by comparing the difference in solar radiation absorbed at the surface  
286 under clear-sky conditions (a model calculation that ignores the influence of clouds).

287

### 288 **3.2 Carbon Cycle and Biogeochemical Warming**

289 In addition to biogeophysical warming, acclimation of leaf mass per area reduced carbon  
290 uptake by the biosphere (Fig. 1c, 3c), which would induce further warming by increasing  
291 atmospheric CO<sub>2</sub> levels. Net primary productivity increased 51% (+30.1 PgC/yr, CI<sub>95%</sub> 29.8 to  
292 30.4) in response to a doubling of CO<sub>2</sub> (CC - CTRL). Acclimation of leaf mass per area strongly  
293 moderated the positive effect of carbon fertilization on net primary productivity in response to  
294 elevated CO<sub>2</sub>, reducing the gain in productivity by -5.8 PgC/yr (CCLMA - CC; CI<sub>95%</sub> -5.5 to -  
295 6.0, Table 1, S2). This decrease in net primary productivity in response to leaf acclimation was  
296 driven by declines in the tropics, followed by the northern extratropics (Table 1, S2).

297 Smaller increases in leaf area and higher temperatures in response to leaf acclimation  
298 both contributed to the reduced gains in productivity relative to the climate change control.  
299 Decreases in gross primary productivity (CCLMA - CC) were best described by a multiple  
300 regression using both changes (CCLMA - CC) in temperature and leaf area as predictors  
301 (multiple regression  $R^2 = 0.32$ , Fig. S2d). Changes in net primary productivity were weakly but  
302 best related to temperature change ( $R^2 = 0.24$ , Fig. S2c).

303 From the reduced gains in  
 304 carbon uptake in response to leaf  
 305 mass per area acclimation we  
 306 estimate a change in global mean  
 307 temperature. Our simulations did  
 308 not directly account for this  
 309 biogeochemical warming, as  
 310 atmospheric CO<sub>2</sub> levels within each  
 311 simulation were held fixed in time.  
 312 Instead, we estimate  
 313 biogeochemical warming (see  
 314 Materials and Methods) associated  
 315 with the net change in carbon  
 316 storage from the difference in  
 317 carbon uptake by vegetation, as  
 318 measured by net primary  
 319 productivity, when leaf acclimation  
 320 is considered (CCLMA - CC). The -  
 321 5.5 to -6.0 PgC/yr reduction in net  
 322 primary productivity gains would  
 323 increase global atmospheric CO<sub>2</sub> concentration by +0.4 to +1.2 ppm/yr when considering the  
 324 effect of oceanic buffering. We estimate that this additional atmospheric CO<sub>2</sub> induces  
 325 biogeochemical warming of +0.1 to +1.0°C over 100 years, the approximate average timescale

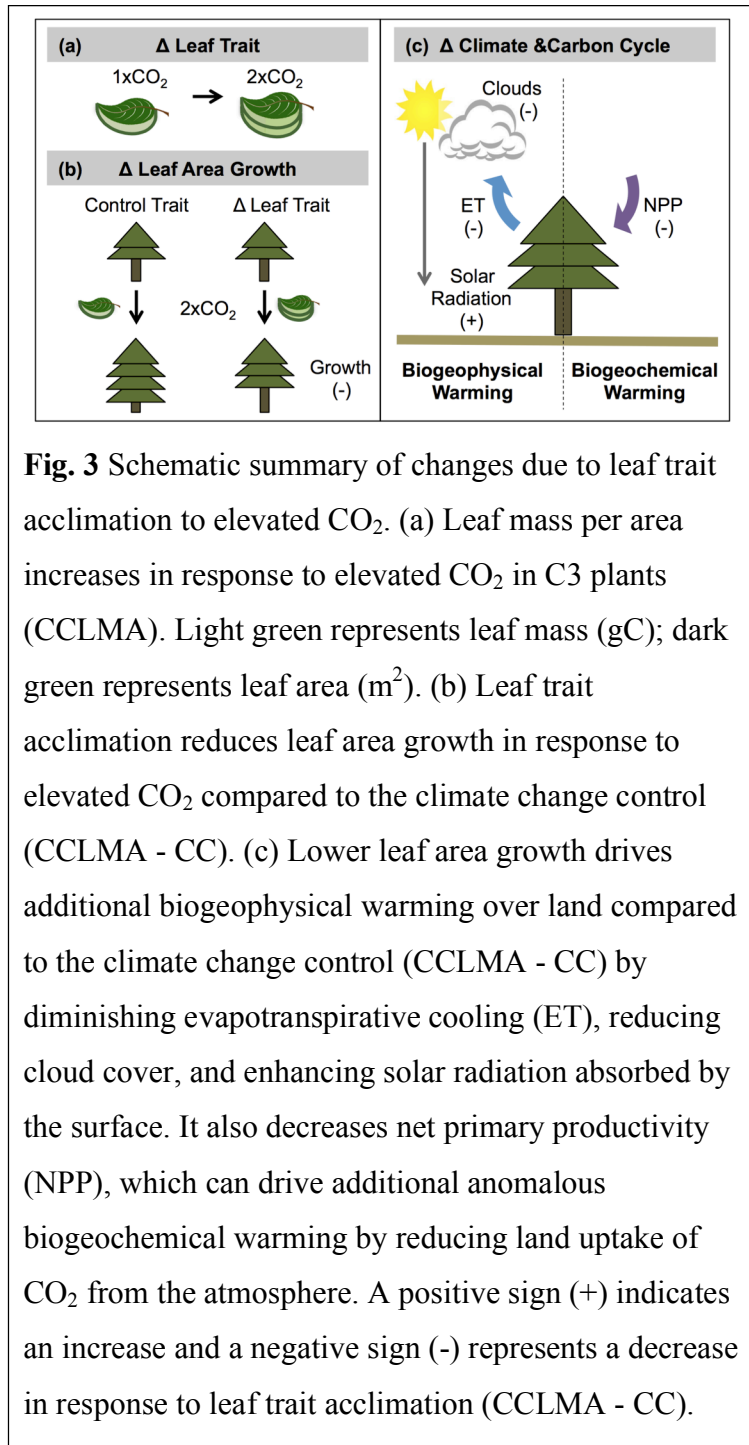


**Fig. 3** Schematic summary of changes due to leaf trait acclimation to elevated CO<sub>2</sub>. (a) Leaf mass per area increases in response to elevated CO<sub>2</sub> in C3 plants (CCLMA). Light green represents leaf mass (gC); dark green represents leaf area (m<sup>2</sup>). (b) Leaf trait acclimation reduces leaf area growth in response to elevated CO<sub>2</sub> compared to the climate change control (CCLMA - CC). (c) Lower leaf area growth drives additional biogeophysical warming over land compared to the climate change control (CCLMA - CC) by diminishing evapotranspirative cooling (ET), reducing cloud cover, and enhancing solar radiation absorbed by the surface. It also decreases net primary productivity (NPP), which can drive additional anomalous biogeochemical warming by reducing land uptake of CO<sub>2</sub> from the atmosphere. A positive sign (+) indicates an increase and a negative sign (-) represents a decrease in response to leaf trait acclimation (CCLMA - CC).

326 for a doubling of CO<sub>2</sub> from 355 to 710ppm under the IPCC RCP8.5 and RCP6 emissions  
327 scenarios (Cubasch et al., 2013). The sum of this biogeochemical warming and the  
328 biogeophysical warming reported above brings the total additional warming due to leaf mass per  
329 area acclimation (CCLMA - CC) to +0.3 to +1.4°C greater than the warming due to a doubling  
330 of CO<sub>2</sub> in the control climate change simulation.

331

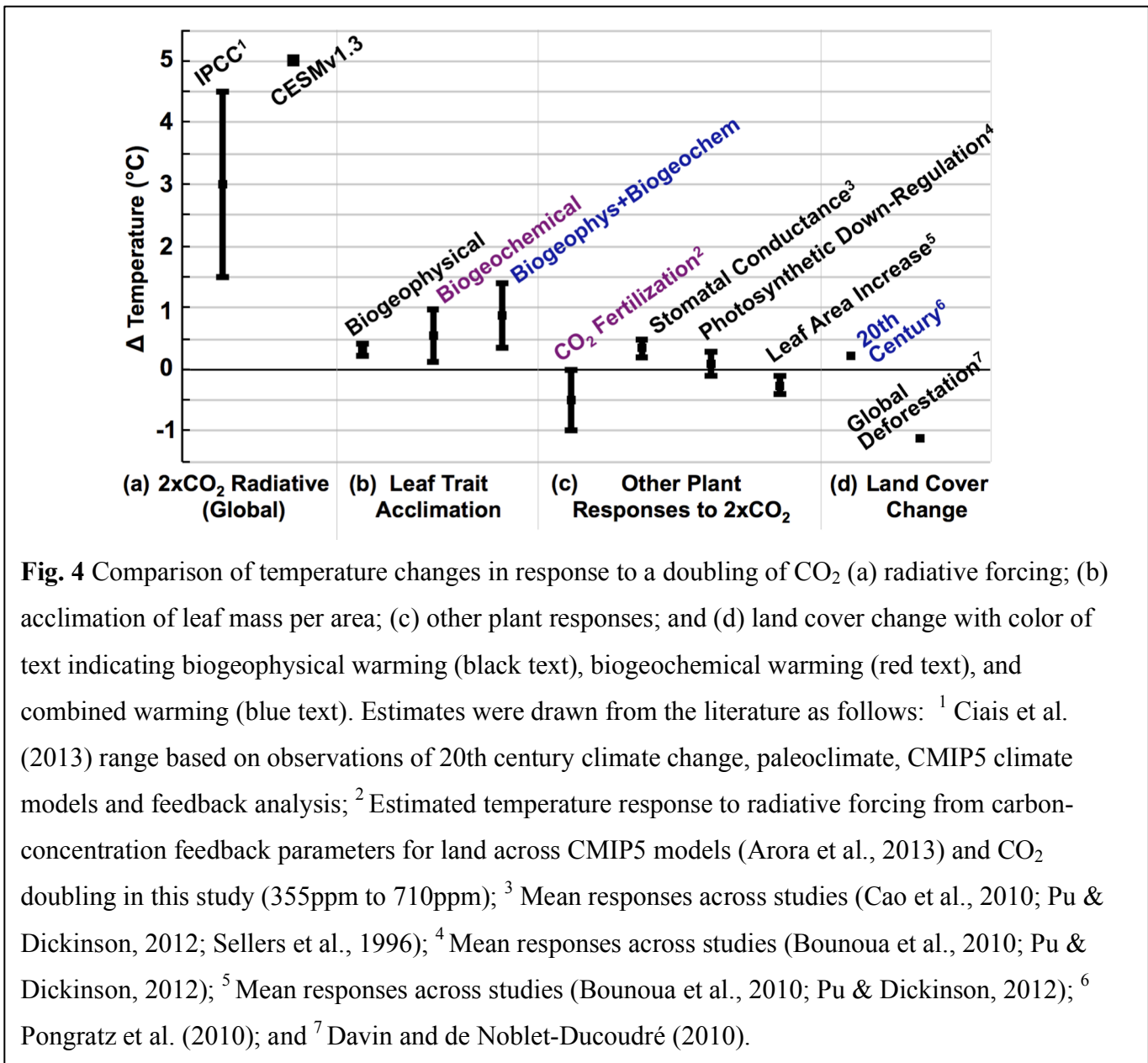
#### 332 **4 Discussion**

333 We find that leaf trait responses could have significant large-scale climate implications.  
334 Increased leaf mass per area enhances warming beyond the direct effects of elevated CO<sub>2</sub> by  
335 moderating evapotranspiration and enhancing absorption of solar radiation, and by lessening the  
336 rise in leaf area which lowers net primary productivity gains (Fig. 3).

337 The surface temperature change in response to leaf trait acclimation is of comparable  
338 magnitude to the climate response to other important climate forcings (Fig. 4). For example, the  
339 enhanced warming in our experiment (+0.3 to +1.4°C) is smaller but of the same order of  
340 magnitude as the change in temperature in response to a doubling of CO<sub>2</sub> estimated by the IPCC  
341 (+1.5 to +4.5°C) from observed 20th century climate change, paleoclimate, feedback analysis,  
342 and climate models (Ciais et al., 2013). While these comparisons are not exact, as the methods  
343 and measures of uncertainty differ, they provide an order of magnitude comparison for our  
344 results. Enhanced warming in our experiment is also of greater or comparable magnitude to the  
345 temperature response to large-scale land cover change (Fig. 4d), such as anthropogenic land  
346 cover change over the 20th century (-0.04°C physical, +0.27 chemical, +0.22 total, over land;  
347 Pongratz et al., 2010) and theoretical global deforestation (-1.1°C biogeophysical over land;  
348 Davin & de Noblet-Ducoudré, 2010).



349 Furthermore, our results show that the surface temperature change in response to leaf trait  
 350 acclimation can exceed or match several well-studied plant physiological feedbacks to elevated  
 351 CO<sub>2</sub> that are included in most climate projections (Fig. 4c). These include the vegetation carbon-  
 352 concentration feedback (0 to -1.0°C; estimated from the change in CO<sub>2</sub> implemented in this  
 353 study of 355ppm to 710ppm and the CMIP5 model range for land carbon-concentration feedback  
 354 parameter from Arora et al., 2013), stomatal conductance response to elevated CO<sub>2</sub> (+0.2 to



355 +0.5°C biogeophysical over land; Betts et al., 1997, 2007; Boucher et al., 2009; Cao et al., 2010;  
356 Cox et al., 1999; Pu & Dickinson, 2012; Sellers et al., 1996); photosynthetic down-regulation (-  
357 0.1 to +0.3 °C biogeophysical over land; Bounoua et al., 2010; Pu & Dickinson, 2012); and  
358 increased leaf area index (+30 to 60%) due to CO<sub>2</sub> fertilization and increased water use  
359 efficiency under elevated CO<sub>2</sub> (-0.1 to -0.4 °C biogeophysical over land; Betts et al., 1997;  
360 Bounoua et al., 2010; Pu & Dickinson, 2012).

361         The reduced increase in terrestrial productivity in response to leaf mass per area  
362 acclimation is on the order of other large-scale carbon cycle perturbations and moderates the  
363 effect of CO<sub>2</sub> fertilization on plant growth and carbon uptake from the atmosphere. The -5.8  
364 PgC/yr (CI<sub>95%</sub> -5.5 to -6.0) reduction in net primary productivity in response to leaf mass per area  
365 acclimation in our simulations (CCLMA - CC) is a reduced carbon sink comparable in  
366 magnitude to current global fossil fuel emissions (8 PgC/yr; Ciais et al., 2013). It is larger than  
367 the total current terrestrial biosphere uptake of CO<sub>2</sub> from the atmosphere (3 PgC/yr; Le Quéré et  
368 al., 2016).

369         Leaf mass per area acclimation to CO<sub>2</sub> represents a shift in the relationship between two  
370 key ecosystem properties - productivity and leaf area. As such, this acclimation will remain  
371 important for climate and carbon cycling if other trait responses further modify estimates of  
372 productivity. Notably, the magnitude of maximum photosynthetic rate (e.g. V<sub>cmax25</sub>, J<sub>max25</sub>)  
373 acclimation to CO<sub>2</sub> remains uncertain and difficult to represent at the global scale (Rogers et al.,  
374 2017; Smith & Dukes, 2013). While most estimates suggest that maximum photosynthetic rates  
375 will decrease in response to CO<sub>2</sub> (Ainsworth & Long, 2005; Leakey et al., 2012; Rogers et al.,  
376 2017; Smith & Dukes, 2013), which would amplify our results, we conservatively do not change  
377 these rates in our primary experiment (CCLMA - CC). We estimate that maximum

378 photosynthetic rates would need to increase (opposite direction of expected CO<sub>2</sub> acclimation) by  
379 one third to bolster net primary productivity enough to offset the biogeophysical warming over  
380 land due to leaf acclimation in our experiments (supporting information Text S2.3). This altered  
381 balance between productivity (biogeochemical warming) and leaf area (biogeophysical warming)  
382 demonstrates the importance of including leaf mass per area acclimation to CO<sub>2</sub>.

383         Longer leaf lifespans are correlated with higher leaf mass per area across species (Wright  
384 et al., 2004) and could be expected to offset the climate influence of leaf mass per area by  
385 enhancing productivity beyond current estimates. However, this correlation observed across  
386 species does not necessarily hold for trait changes within a species, such as in response to  
387 acclimation (Anderegg, 2017; Fisher et al., 2015; Lusk et al., 2008). Observations of leaf lifespan  
388 acclimation to elevated CO<sub>2</sub> indicate that the response is highly variable in magnitude and sign,  
389 and inconsistently associated with higher leaf mass per area (e.g. Norby et al., 2003, 2010;  
390 Taylor et al., 2008 and references therein). As the observational evidence does not support an  
391 increase in leaf lifespan in coordination with leaf mass per area acclimation to CO<sub>2</sub>, we chose not  
392 to impose this change in our simulations. However, we do include changes in leaf area duration  
393 due to phenological responses to warming temperature and soil moisture in all simulations  
394 (Oleson et al., 2013).

395         Several environmental drivers of leaf mass per area acclimation - CO<sub>2</sub>, temperature, and  
396 nutrient limitation - will likely be modified by climate change. We estimate that the influence of  
397 temperature acclimation of leaf mass per area globally is secondary to CO<sub>2</sub> (supporting  
398 information Text S2.1, Fig. S1). The effect of temperature warming on leaf mass per area occurs  
399 under cold conditions, thus the acclimation is limited to high latitude boreal regions (Fig. S5).  
400 Nutrient limitation is expected to increase with CO<sub>2</sub> fertilization of plant growth (Norby et al.,

401 2010; Wieder et al., 2015) and has been found to enhance leaf mass per area in manipulation  
402 experiments (Poorter et al., 2009), which could further amplify the impacts of leaf acclimation to  
403 elevated CO<sub>2</sub>. The magnitude of leaf mass per area acclimation in response to climate change  
404 may ultimately depend upon the combined influence, including potential interaction effects, of  
405 multiple climate drivers.

406 Accounting for leaf acclimation in climate projections will require the ability to represent  
407 the functional relationship between leaf mass per area and its climate drivers, especially CO<sub>2</sub>, by  
408 biome at the global scale. This remains challenging (Medlyn et al., 2015). Poorter et al. (2009)'s  
409 empirical relationship, used herein, shows that on average leaf mass per area increases with CO<sub>2</sub>  
410 in C<sub>3</sub> species. However, the proportion of variance in the magnitude of acclimation explained by  
411 this relationship is relatively low (Poorter et al., 2009), suggesting that other key drivers, such as  
412 plant type, still need to be incorporated. A mechanistic model of leaf mass per area acclimation  
413 also remains elusive. The leading hypothesis for why elevated CO<sub>2</sub> increases leaf mass per area  
414 is that the abundance of carbon causes nonstructural carbohydrates to accumulate in leaves  
415 (Poorter et al., 2009, 1997; Pritchard et al., 1999; Roumet et al., 1999). One possible advantage  
416 for plants of increasing leaf mass per area under elevated CO<sub>2</sub> is that it maintains a high level of  
417 leaf nitrogen per leaf area (g N / m<sup>2</sup> leaf area), an essential component of photosynthetic  
418 machinery, by counteracting a decrease in leaf nitrogen concentration (g N / g leaf) driven by  
419 larger pools of nonstructural carbohydrates (N per area = N per mass x leaf mass per area)  
420 (Ishizaki et al., 2003; Luo et al., 1994; Peterson et al., 1999; Poorter et al., 1997; Stitt & Krapp,  
421 1999). However, this process operates differently across environments, plant species, and even  
422 genotypes (Körner et al., 1997; Luo et al., 1994; Peterson et al., 1999; Poorter et al., 1997, 2009;  
423 Pritchard et al., 1999; Roumet et al., 1999; Stitt & Krapp, 1999). Further research into the

424 underlying mechanism, influences of multiple environmental drivers, and differences in  
425 acclimation between plant types is needed to develop a representation of leaf mass per area  
426 acclimation suitable for use in Earth system models.

427         The climate implications of increased leaf mass per area reveal an urgent need for  
428 observational constraints on the magnitude and mechanism of leaf trait acclimation to future  
429 climate conditions. Other structural trait acclimations that influence leaf area may have similar  
430 climate implications that require testing. Our findings suggest that the uncertainty in vegetation-  
431 climate feedbacks, and therefore climate change projections, is even larger than previously  
432 thought.

433

#### 434 **Acknowledgements**

435 We thank M. Laguë and E. Garcia for help with model set up. We acknowledge National Science  
436 Foundation Awards AGS-1321745 and AGS-1553715 to the University of Washington. High-  
437 performance computing support from Yellowstone (ark:/85065/d7wd3xhc) was provided by  
438 NCAR's Computational and Information Systems Laboratory, sponsored by the National Science  
439 Foundation. M.K. thanks the UW Program on Climate Change Graduate Fellowship for support.  
440 Model results to be made available from University of Washington library archive at publication.

441

#### 442 **References**

443 Ainsworth, E. A., & Long, S. P. (2005). What have we learned from 15 years of free-air CO<sub>2</sub>  
444 enrichment (FACE)? A meta-analytic review of the responses of photosynthesis, canopy  
445 properties and plant production to rising CO<sub>2</sub>. *New Phytologist*, *165*(2), 351–371.  
446 <https://doi.org/10.1111/j.1469-8137.2004.01224.x>

447 Ainsworth, E. A., & Rogers, A. (2007). The response of photosynthesis and stomatal  
448 conductance to rising [CO<sub>2</sub>]: mechanisms and environmental interactions. *Plant, Cell and*  
449 *Environment*, *30*, 258–270. <https://doi.org/10.1111/j.1365-3040.2007.01641.x>

- 450 Anderegg, L. D. L. (2017). On the variation of traits and tree range constraints, (Doctoral  
451 dissertation). Retrieved from University of Washington Libraries ResearchWorks Service.  
452 (<http://hdl.handle.net/1773/39962>). Seattle, WA: University of Washington.
- 453 Archer, D., Eby, M., Brovkin, V., Ridgwell, A., Cao, L., Mikolajewicz, U., et al. (2009).  
454 Atmospheric Lifetime of Fossil Fuel Carbon Dioxide. *Annual Review of Earth and Planetary*  
455 *Sciences*, 37(1), 117–134. <https://doi.org/10.1146/annurev.earth.031208.100206>
- 456 Arora, V. K., Boer, G. J., Friedlingstein, P., & Eby, M. (2013). Carbon–concentration and  
457 carbon–climate feedbacks in CMIP5 Earth system models. *Journal of Climate*, 26(15),  
458 5289–5314. <https://doi.org/10.1175/JCLI-D-12-00494.1>
- 459 Betts, R. A., Boucher, O., Collins, M., Cox, P. M., Falloon, P. D., Gedney, N., et al. (2007).  
460 Projected increase in continental runoff due to plant responses to increasing carbon dioxide.  
461 *Nature*, 448(7157), 1037–1041. <https://doi.org/10.1038/nature06045>
- 462 Betts, R. A., Cox, P. M., Lee, S. E., & Woodward, F. I. (1997). Contrasting physiological and  
463 structural vegetation feedbacks in climate change simulations. *Nature*, 387(6635), 796–799.  
464 <https://doi.org/10.1038/42924>
- 465 Bonan, G. B. (2008). Forests and climate change: forcings, feedbacks, and the climate benefits of  
466 forests. *Science*, 320, 1444–1449. <https://doi.org/10.1126/science.1155121>
- 467 Boucher, O., Jones, A., & Betts, R. A. (2009). Climate response to the physiological impact of  
468 carbon dioxide on plants in the Met Office Unified Model HadCM3. *Climate Dynamics*,  
469 32(2-3), 237–249. <https://doi.org/10.1007/s00382-008-0459-6>
- 470 Bounoua, L., Hall, F. G., Sellers, P. J., Kumar, A., Collatz, G. J., Tucker, C. J., & Imhoff, M. L.  
471 (2010). Quantifying the negative feedback of vegetation to greenhouse warming: A  
472 modeling approach. *Geophysical Research Letters*, 37(23).  
473 <https://doi.org/10.1029/2010GL045338>
- 474 Broecker, W. S., Takahashi, T., Simpson, H. J., & Peng, T. H. (1979). Fate of Fossil Fuel Carbon  
475 Dioxide and the Global Carbon Budget. *Science*, 206(4417), 409–418.  
476 <https://doi.org/10.1126/science.206.4417.409>
- 477 Cao, L., Bala, G., Caldeira, K., Nemani, R., & Ban-Weiss, G. (2010). Importance of carbon  
478 dioxide physiological forcing to future climate change. *Proceedings of the National*  
479 *Academy of Sciences of the United States of America*, 107(21), 9513–9518.  
480 <https://doi.org/10.1073/pnas.0913000107>
- 481 Ciais, P., Sabine, C., Bala, G., Bopp, L., Brovkin, V., Canadell, J., et al. (2013). Carbon and  
482 Other Biogeochemical Cycles. In *Climate change 2013: the physical science basis.*  
483 *Contribution of Working Group I to the Fifth Assessment Report of the Intergovernmental*  
484 *Panel on Climate Change* (pp. 465–570). Cambridge University Press.
- 485 Cox, P. M., Betts, R. A., Bunton, C. B., Essery, R., Rowntree, P. R., & Smith, J. (1999). The  
486 impact of new land surface physics on the GCM simulation of climate and climate

- 487 sensitivity. *Climate Dynamics*, 15(3), 183–203. <https://doi.org/10.1007/s003820050276>
- 488 Cubasch, U., Wuebbles, D., Chen, D., Facchini, M. C., Frame, D., Mahowald, N., & Winther, J.  
489 G. (2013). Introduction. In T. F. Stocker, D. Qin, G. K. Plattner, M. Tignor, S. K. Allen, J.  
490 Boschung, et al. (Eds.), *Climate Change 2013: The Physical Science Basis. Contribution of*  
491 *Working Group I to the Fifth Assessment Report of the Intergovernmental Panel on Climate*  
492 *Change* (pp. 121–158). Cambridge, UK: Cambridge University Press.
- 493 Davin, E. L., & de Noblet-Ducoudré, N. (2010). Climatic Impact of Global-Scale Deforestation:  
494 Radiative versus Nonradiative Processes. *Journal of Climate*, 23(1), 97–112.  
495 <https://doi.org/10.1175/2009JCLI3102.1>
- 496 De Kauwe, M. G., Medlyn, B. E., Zaehle, S., Walker, A. P., Dietze, M. C., Hickler, T., et al.  
497 (2013). Forest water use and water use efficiency at elevated CO<sub>2</sub>: a model-data  
498 intercomparison at two contrasting temperate forest FACE sites. *Global Change Biology*,  
499 19(6), 1759–1779. <https://doi.org/10.1111/gcb.12164>
- 500 De Kauwe, M. G., Medlyn, B. E., Zaehle, S., Walker, A. P., Dietze, M. C., Wang, Y.-P., et al.  
501 (2014). Where does the carbon go? A model-data intercomparison of vegetation carbon  
502 allocation and turnover processes at two temperate forest free-air CO<sub>2</sub> enrichment sites. *New*  
503 *Phytologist*, 203(3), 883–899. <https://doi.org/10.1111/nph.12847>
- 504 Efron, B., & Gong, G. (1983). A Leisurely Look at the Bootstrap, the Jackknife, and Cross-  
505 Validation. *The American Statistician*, 37(1), 36–48. <https://doi.org/10.2307/2685844>
- 506 Efron, B., & Tibshirani, R. J. (1994). An introduction to the bootstrap. CRC press.
- 507 Fisher, R. A., Muszala, S., Verstein, M., Lawrence, P., Xu, C., McDowell, N. G., et al.  
508 (2015). Taking off the training wheels: the properties of a dynamic vegetation model without  
509 climate envelopes. *Geoscientific Model Development Discussions*, 8(4), 3293–3357.  
510 <https://doi.org/10.5194/gmdd-8-3293-2015>
- 511 Friedlingstein, P., Meinshausen, M., Arora, V. K., Jones, C. D., Anav, A., Liddicoat, S. K., &  
512 Knutti, R. (2014). Uncertainties in CMIP5 Climate Projections due to Carbon Cycle  
513 Feedbacks. *Journal of Climate*, 27(2), 511–526. <https://doi.org/10.1175/JCLI-D-12-00579.1>
- 514 Hansen, J. E., Sato, M., Lacis, A., Ruedy, R., Tegen, I., & Matthews, E. (1998). Climate forcings  
515 in the Industrial era. *Proceedings of the National Academy of Sciences of the United States of*  
516 *America*, 95(22), 12753–12758. <https://doi.org/10.1073/pnas.95.22.12753>
- 517 Hunke, E. C., & Lipscomb, W. H. (2010). CICE: the Los Alamos Sea Ice Model Documentation  
518 and Software User's Manual Version 4.1 LA-CC-06-012, 1–76.
- 519 Ishizaki, S., Hikosaka, K., & Hirose, T. (2003). Increase in leaf mass per area benefits plant  
520 growth at elevated CO<sub>2</sub> concentration. *Annals of Botany*, 91(7), 905–914.  
521 <https://doi.org/10.1093/aob/mcg097>
- 522 Kattge, J., & Knorr, W. (2007). Temperature acclimation in a biochemical model of

- 523 photosynthesis: a reanalysis of data from 36 species. *Plant, Cell and Environment*, 30(9),  
524 1176–1190. <https://doi.org/10.1111/j.1365-3040.2007.01690.x>
- 525 Kattge, J., Diaz, S., Lavorel, S., Prentice, I. C., Leadley, P., Bonisch, G., et al. (2011). TRY—a  
526 global database of plant traits. *Global Change Biology*, 17, 2905–2935.  
527 <https://doi.org/10.1111/j.1365-2486.2011.02451.x>
- 528 Koven, C. D., Lawrence, D. M., & Riley, W. J. (2015). Permafrost carbon–climate feedback is  
529 sensitive to deep soil carbon decomposability but not deep soil nitrogen dynamics.  
530 *Proceedings of the National Academy of Sciences of the United States of America*, 112(12),  
531 3752–3757. <https://doi.org/10.1073/pnas.1415123112>
- 532 Körner, C., Diemer, M., Schäppi, B., Niklaus, P., & Arnone, J. (1997). The responses of alpine  
533 grassland to four seasons of CO<sub>2</sub> enrichment: a synthesis. *Acta Oecologica*, 18(3), 165–175.  
534 [https://doi.org/10.1016/S1146-609X\(97\)80002-1](https://doi.org/10.1016/S1146-609X(97)80002-1)
- 535 Le Quéré, C., Andrew, R. M., Canadell, J. G., Sitch, S., Korsbakken, J. I., Peters, G. P., et al.  
536 (2016). Global Carbon Budget 2016. *Earth System Science Data*, 8(2), 605–649.  
537 <https://doi.org/10.5194/essd-8-605-2016>
- 538 Leakey, A. D. B., Ainsworth, E. A., Bernacchi, C. J., Zhu, X., Long, S. P., & Ort, D. R. (2012).  
539 Photosynthesis in a CO<sub>2</sub>-Rich Atmosphere. In *Photosynthesis in silico* (Vol. 34, pp. 733–  
540 768). Dordrecht: Springer Netherlands. [https://doi.org/10.1007/978-94-007-1579-0\\_29](https://doi.org/10.1007/978-94-007-1579-0_29)
- 541 Lombardozzi, D. L., Bonan, G. B., Smith, N. G., Dukes, J. S., & Fisher, R. A. (2015).  
542 Temperature acclimation of photosynthesis and respiration: A key uncertainty in the carbon  
543 cycle-climate feedback. *Geophysical Research Letters*, 42(20), 8624–8631.  
544 <https://doi.org/10.1002/2015GL065934>
- 545 Lovenduski, N. S., & Bonan, G. B. (2017). Reducing uncertainty in projections of terrestrial  
546 carbon uptake. *Environmental Research Letters*, 12(4), 044020.  
547 <https://doi.org/10.1088/1748-9326/aa66b8>
- 548 Luo, Y., Field, C. B., & Mooney, H. A. (1994). Predicting responses of photosynthesis and root  
549 fraction to elevated [CO<sub>2</sub>]: interactions among carbon, nitrogen, and growth. *Plant, Cell  
550 and Environment*, 17(11), 1195–1204. <https://doi.org/10.1111/j.1365-3040.1994.tb02017.x>
- 551 Lusk, C. H., Reich, P. B., Montgomery, R. A., Ackerly, D. D., & Cavender-Bares, J. (2008).  
552 Why are evergreen leaves so contrary about shade? *Trends in Ecology & Evolution*, 23(6),  
553 299–303. <https://doi.org/10.1016/j.tree.2008.02.006>
- 554 Mahowald, N., Lo, F., Zheng, Y., Harrison, L., Funk, C., Lombardozzi, D., & Goodale, C.  
555 (2016). Projections of leaf area index in earth system models. *Earth System Dynamics*, 7(1),  
556 211–229. <https://doi.org/10.5194/esd-7-211-2016>
- 557 Medlyn, B. E., Badeck, F. W., De Pury, D., Barton, C., Broadmeadow, M., Ceulemans, R., et al.  
558 (1999). Effects of elevated [CO<sub>2</sub>] on photosynthesis in European forest species: a meta-



- 559 analysis of model parameters. *Plant, Cell and Environment*, 22(12), 1475–1495.  
560 <https://doi.org/10.1046/j.1365-3040.1999.00523.x>
- 561 Medlyn, B. E., Zaehle, S., De Kauwe, M. G., Walker, A. P., Dietze, M. C., Hanson, P. J., et al.  
562 (2015). Using ecosystem experiments to improve vegetation models. *Nature Climate*  
563 *Change*, 5(6), 528–534. <https://doi.org/10.1038/nclimate2621>
- 564 Myhre, G., Highwood, E. J., Shine, K. P., & Stordal, F. (1998). New estimates of radiative  
565 forcing due to well mixed greenhouse gases. *Geophysical Research Letters*, 25(14), 2715–  
566 2718. <https://doi.org/10.1029/98GL01908>
- 567 Neale, R. B., Chen, C.-C., Gettelman, A., Lauritzen, P. H., Park, S., Williamson, D. L.,  
568 Coauthors. (2012). Description of the NCAR Community Atmosphere Model (CAM 5.0).  
569 NCAR Technical Note. NCAR/TN-486+STR, 1–289.
- 570 Niinemets, Ü. (2001). Global-scale climatic controls of leaf dry mass per area, density, and  
571 thickness in trees and shrubs. *Ecology*, 82(2), 453–469. [https://doi.org/10.1890/0012-9658\(2001\)082\[0453:GSCCOL\]2.0.CO;2](https://doi.org/10.1890/0012-9658(2001)082[0453:GSCCOL]2.0.CO;2)
- 573 Norby, R. J., Sholtis, J. D., Gunderson, C. A., & Jawdy, S. S. (2003). Leaf dynamics of a  
574 deciduous forest canopy: no response to elevated CO<sub>2</sub>. *Oecologia*, 136(4), 574–584.  
575 <https://doi.org/10.1007/s00442-003-1296-2>
- 576 Norby, R. J., Warren, J. M., Iversen, C. M., Medlyn, B. E., & McMurtrie, R. E. (2010). CO<sub>2</sub>  
577 enhancement of forest productivity constrained by limited nitrogen availability. *Proceedings*  
578 *of the National Academy of Sciences of the United States of America*, 107(45), 19368–19373.  
579 <https://doi.org/10.1073/pnas.1006463107>
- 580 Oleson, K. W., Lawrence, D. M., Bonan, G. B., Drewniak, B., Huang, M., Koven, C. D., et al.  
581 (2013). Technical Description of the version 4.5 of the Community Land Model (CLM).  
582 NCAR Technical Note. NCAR/TN-503+STR. Retrieved from  
583 [http://www.cesm.ucar.edu/models/cesm1.2/clm/CLM45\\_Tech\\_Note.pdf](http://www.cesm.ucar.edu/models/cesm1.2/clm/CLM45_Tech_Note.pdf)
- 584 Patton, A. (2007). Automatic Block Length Selection Procedure. Retrieved June 28, 2016, from  
585 [http://public.econ.duke.edu/~ap172/opt\\_block\\_length\\_REV\\_dec07.txt](http://public.econ.duke.edu/~ap172/opt_block_length_REV_dec07.txt)
- 586 Patton, A., Politis, D. N., & White, H. (2009). Correction to “Automatic block-length selection  
587 for the dependent bootstrap” by D. Politis and H. White. *Econometric Reviews*.  
588 <https://doi.org/10.1080/07474930802459016>
- 589 Pavlick, R., Drewry, D. T., Bohn, K., Reu, B., & Kleidon, A. (2013). The Jena Diversity-  
590 Dynamic Global Vegetation Model (JeDi-DGVM): a diverse approach to representing  
591 terrestrial biogeography and biogeochemistry based on plant functional trade-offs.  
592 *Biogeosciences*, 10(6), 4137–4177. <https://doi.org/10.5194/bg-10-4137-2013>
- 593 Peterson, A. G., Ball, J. T., Luo, Y., Field, C. B., Curtis, P. S., Griffin, K. L., et al. (1999).  
594 Quantifying the response of photosynthesis to changes in leaf nitrogen content and leaf mass  
595 per area in plants grown under atmospheric CO<sub>2</sub> enrichment. *Plant, Cell and Environment*,

- 596 22(9), 1109–1119. <https://doi.org/10.1046/j.1365-3040.1999.00489.x>
- 597 Politis, D. N., & Romano, J. P. (1994). The Stationary Bootstrap. *Journal of the American*  
598 *Statistical Association*, 89(428), 1303–1313. <https://doi.org/10.2307/2290993>
- 599 Politis, D. N., & White, H. (2004). Automatic Block-Length Selection for the Dependent  
600 Bootstrap. *Econometric Reviews*, 23(1), 53–70. <https://doi.org/10.1081/ETC-120028836>
- 601 Pongratz, J., Reick, C. H., Raddatz, T., & Claussen, M. (2010). Biogeophysical versus  
602 biogeochemical climate response to historical anthropogenic land cover change. *Geophysical*  
603 *Research Letters*, 37, L08702. <https://doi.org/10.1029/2010GL043010>
- 604 Poorter, H., Berkel, Y. V., Baxter, R., Hertog, J. D., Dijkstra, P., Gifford, R. M., et al. (1997).  
605 The effect of elevated CO<sub>2</sub> on the chemical composition and construction costs of leaves of  
606 27 C<sub>3</sub> species. *Plant, Cell and Environment*, 20(4), 472–482. <https://doi.org/10.1046/j.1365-3040.1997.d01-84.x>
- 608 Poorter, H., Niinemets, Ü., Poorter, L., Wright, I. J., & Villar, R. (2009). Causes and  
609 consequences of variation in leaf mass per area (LMA): a meta-analysis. *New Phytologist*,  
610 182, 565–588. <https://doi.org/10.1111/j.1469-8137.2009.02830.x>
- 611 Pritchard, S. H., Rogers, H. O., Prior, S. A., & Peterson, C. M. (1999). Elevated CO<sub>2</sub> and plant  
612 structure: a review. *Global Change Biology*, 5(7), 807–837. <https://doi.org/10.1046/j.1365-2486.1999.00268.x>
- 614 Pu, B., & Dickinson, R. E. (2012). Examining vegetation feedbacks on global warming in the  
615 Community Earth System Model. *Journal of Geophysical Research*, 117, D20110.  
616 <https://doi.org/10.1029/2012JD017623>
- 617 Quilis, E. M. (2015). Bootstrapping Time Series. Version 1.0. Retrieved June 17, 2016, from  
618 <https://www.mathworks.com/matlabcentral/fileexchange/53701-bootstrapping-time-series>
- 619 Reich, P. B., Rich, R. L., Lu, X., Wang, Y.-P., & Oleksyn, J. (2014). Biogeographic variation in  
620 evergreen conifer needle longevity and impacts on boreal forest carbon cycle projections.  
621 *Proceedings of the National Academy of Sciences of the United States of America*, 111(38),  
622 13703–13708. <https://doi.org/10.1073/pnas.1216054110>
- 623 Reichstein, M., Bahn, M., Mahecha, M. D., Kattge, J., & Baldocchi, D. D. (2014). Linking plant  
624 and ecosystem functional biogeography. *Proceedings of the National Academy of Sciences of*  
625 *the United States of America*, 111(38), 13697–13702.  
626 <https://doi.org/10.1073/pnas.1216065111>
- 627 Rogers, A., Medlyn, B. E., Dukes, J. S., Bonan, G., Caemmerer, von, S., Dietze, M. C., et al.  
628 (2017). A roadmap for improving the representation of photosynthesis in Earth system  
629 models. *The New Phytologist*, 213(1), 22–42. <https://doi.org/10.1111/nph.14283>
- 630 Roumet, C., Laurent, G., & Roy, J. (1999). Leaf structure and chemical composition as affected  
631 by elevated CO<sub>2</sub>: genotypic responses of two perennial grasses. *New Phytologist*, 143(1),

- 632 73–81. <https://doi.org/10.1046/j.1469-8137.1999.00437.x>
- 633 Said, S. E., & Dickey, D. A. (1984). Testing for Unit Roots in Autoregressive-Moving Average  
634 Models of Unknown Order. *Biometrika*, 71(3), 599–607.  
635 <https://doi.org/10.1093/biomet/71.3.599>
- 636 Scheiter, S., Langan, L., & Higgins, S. I. (2013). Next-generation dynamic global vegetation  
637 models: learning from community ecology. *New Phytologist*, 198(3), 957–969.  
638 <https://doi.org/10.1111/nph.12210>
- 639 Sellers, P. J., Bounoua, L., Collatz, G. J., Randall, D. A., Dazlich, D. A., Los, S. O., et al. (1996).  
640 Comparison of radiative and physiological effects of doubled atmospheric CO<sub>2</sub> on climate.  
641 *Science*, 271(5254), 1402–1406. <https://doi.org/10.1126/science.271.5254.1402>
- 642 Smith, N. G., & Dukes, J. S. (2013). Plant respiration and photosynthesis in global-scale models:  
643 incorporating acclimation to temperature and CO<sub>2</sub>. *Global Change Biology*, 19(1), 45–63.  
644 <https://doi.org/10.1111/j.1365-2486.2012.02797.x>
- 645 Smith, N. G., Lombardozzi, D., Tawfik, A., Bonan, G., & Dukes, J. S. (2017). Biophysical  
646 consequences of photosynthetic temperature acclimation for climate. *Journal of Advances in*  
647 *Modeling Earth Systems*. <https://doi.org/10.1002/2016MS000732>
- 648 Stitt, M., & Krapp, A. (1999). The interaction between elevated carbon dioxide and nitrogen  
649 nutrition: the physiological and molecular background. *Plant, Cell and Environment*, 22(6),  
650 583–621. <https://doi.org/10.1046/j.1365-3040.1999.00386.x>
- 651 Swann, A. L. S., Hoffman, F. M., Koven, C. D., & Randerson, J. T. (2016). Plant responses to  
652 increasing CO<sub>2</sub> reduce estimates of climate impacts on drought severity. *Proceedings of the*  
653 *National Academy of Sciences of the United States of America*, 113(36), 10019–10024.  
654 <https://doi.org/10.1073/pnas.1604581113>
- 655 Taylor, G., Tallis, M. J., Giardina, C. P., Percy, K. E., Miglietta, F., Gupta, P. S., et al. (2008).  
656 Future atmospheric CO<sub>2</sub> leads to delayed autumnal senescence. *Global Change Biology*,  
657 14(2), 264–275. <https://doi.org/10.1111/j.1365-2486.2007.01473.x>
- 658 Van Bodegom, P. M., Douma, J. C., Witte, J. P. M., Ordoñez, J. C., Bartholomeus, R. P., &  
659 Aerts, R. (2012). Going beyond limitations of plant functional types when predicting global  
660 ecosystem-atmosphere fluxes: exploring the merits of traits-based approaches. *Global*  
661 *Ecology and Biogeography*, 21(6), 625–636. [https://doi.org/10.1111/j.1466-](https://doi.org/10.1111/j.1466-8238.2011.00717.x)  
662 [8238.2011.00717.x](https://doi.org/10.1111/j.1466-8238.2011.00717.x)
- 663 Verheijen, L. M., Aerts, R., Brovkin, V., Cavender-Bares, J., Cornelissen, J. H. C., Kattge, J., &  
664 van Bodegom, P. M. (2015). Inclusion of ecologically based trait variation in plant  
665 functional types reduces the projected land carbon sink in an earth system model. *Global*  
666 *Change Biology*, 21(8), 3074–3086. <https://doi.org/10.1111/gcb.12871>
- 667 Verheijen, L. M., Brovkin, V., Aerts, R., Bonisch, G., Cornelissen, J. H. C., Kattge, J., et al.

668 (2013). Impacts of trait variation through observed trait–climate relationships on  
669 performance of an Earth system model: a conceptual analysis. *Biogeosciences*, 10(8), 5497–  
670 5515. <https://doi.org/10.5194/bg-10-5497-2013>

671 Way, D. A., Oren, R., & Kroner, Y. (2015). The space-time continuum: the effects of elevated  
672 CO<sub>2</sub> and temperature on trees and the importance of scaling. *Plant, Cell and Environment*,  
673 38(6), 991–1007. <https://doi.org/10.1111/pce.12527>

674 Wei, Z., Yoshimura, K., Wang, L., Miralles, D. G., Jasechko, S., & Lee, X. (2017). Revisiting  
675 the contribution of transpiration to global terrestrial evapotranspiration. *Geophysical*  
676 *Research Letters*, 44(6), 2792–2801. <https://doi.org/10.1002/2016GL072235>

677 White, M. A., Thornton, P. E., Running, S. W., & Nemani, R. R. (2000). Parameterization and  
678 sensitivity analysis of the BIOME-BGC terrestrial ecosystem model: net primary production  
679 controls. *Earth Interactions*, 4(3), 1–85. [https://doi.org/10.1175/1087-  
680 3562\(2000\)004<0003:PASAOT>2.0.CO;2](https://doi.org/10.1175/1087-3562(2000)004<0003:PASAOT>2.0.CO;2)

681 Wieder, W. R., Cleveland, C. C., Smith, W. K., & Todd-Brown, K. (2015). Future productivity  
682 and carbon storage limited by terrestrial nutrient availability. *Nature*, 8(6), 441–444.  
683 <https://doi.org/10.1038/ngeo2413>

684 Wright, I. J., Reich, P. B., Westoby, M., Ackerly, D. D., Baruch, Z., Bongers, F., et al. (2004).  
685 The worldwide leaf economics spectrum. *Nature*, 428(6985), 821–827.  
686 <https://doi.org/10.1038/nature02403>

687 Zhou, B., & Wong, W. H. (2011). A Bootstrap-Based Non-Parametric Anova Method with  
688 Applications to Factorial Microarray Data. *Statistica Sinica*, 21(2), 495–514.  
689 <https://doi.org/10.5705/ss.2011.023a>

1  
2  
3  
4  
5  
6  
7  
8  
9  
10  
11  
12  
13  
14  
15  
16  
17  
18

**Supporting Information for**

**Leaf trait acclimation amplifies simulated climate warming  
in response to elevated carbon dioxide.**

Marlies Kovenock<sup>1</sup> and Abigail L.S. Swann<sup>2,1</sup>

<sup>1</sup>Department of Biology, University of Washington, Box 351800, Seattle, WA 98195,  
USA

<sup>2</sup>Department of Atmospheric Sciences, University of Washington, Box 351640, Seattle,  
WA 98195, USA

**Contents of this file**

Text S1 to S2

Figures S1 to S5

Tables S1 to S2

19 **Text S1. Materials and Methods**

20 **1.1 Nitrogen Cycle**

21 As the default model's interactive nitrogen cycle breaks the relationship between  
22 transpiration fluxes and gross primary productivity (De Kauwe et al., 2013) we disabled  
23 it and represented nitrogen limitation with a fractional reduction in the rate of  
24 photosynthesis for each plant functional type following the methods of Koven et al.  
25 (2015).

26  
27 **1.2 CO<sub>2</sub> Acclimation of Leaf Mass per Area Estimation and Implementation**

28 We estimated the plausible extent of leaf mass per area acclimation using Poorter  
29 et al. (2009)'s meta-analysis of approximately 200 studies of leaf mass per area response  
30 to CO<sub>2</sub> level. Specifically, we added the approximate interquartile range for the response  
31 of leaf mass per area to a doubling of CO<sub>2</sub> in all plants (no interquartile range for C<sub>3</sub>  
32 plants was reported) to the median response for C<sub>3</sub> plants. The resulting level of change, a  
33 one third increase in leaf mass per area, was implemented by directly modifying the  
34 model parameter controlling leaf mass per area at the top of the canopy. This model  
35 parameter, SLA<sub>O</sub>, represents specific leaf area (m<sup>2</sup> leaf area/g leaf carbon), the inverse of  
36 leaf mass per area. We therefore multiplied the SLA<sub>O</sub> parameter for all C<sub>3</sub> plant types by  
37 0.75 to implement a one third increase in leaf mass per area.

38 As formulated by default, increasing leaf mass per area in this Earth system model  
39 raises area-based maximum photosynthetic rates (μmol/m<sup>2</sup>/s) as follows:

40  
41 
$$V_{\text{cmax25}} = \alpha \text{ LMA} / \text{CN}_L \quad (\text{Eqn 1})$$
  
42

43 where  $V_{\text{cmax25}}$  is the maximum rate of carboxylation at 25° C (μmol C/m<sup>2</sup>/s), LMA is the  
44 leaf mass per area (gC/m<sup>2</sup> leaf area), CN<sub>L</sub> is the leaf carbon-to-nitrogen ratio (gC/gN),  
45 and  $\alpha$  accounts for the amount of nitrogen in Rubisco and the specific activity of Rubisco.  
46 Other area-based maximum photosynthetic rate parameters ( $J_{\text{max25}}$ ,  $T_{\text{p25}}$ ) are calculated in  
47 proportion to  $V_{\text{cmax25}}$ . In all but one simulation (CCLMAPS), we maintained control  
48 levels of area-based maximum photosynthetic rates by increasing the parameter values  
49 for CN<sub>L</sub> (leaf gC/gN) for each C<sub>3</sub> plant type by one third. This change encompasses  
50 decreases in both CN<sub>L</sub> and the fraction of nitrogen in Rubisco, which have been observed  
51 in response to elevated CO<sub>2</sub> in manipulation experiments (reviewed in Ainsworth &  
52 Long, 2005; Leakey et al., 2012; Way et al., 2015). Prior studies have identified trait-  
53 climate relationships in the literature that suggest that  $V_{\text{cmax25}}$  and  $J_{\text{max25}}$  decrease with  
54 CO<sub>2</sub> (Ainsworth & Rogers, 2007; Medlyn et al., 1999). However, estimating an exact  
55 magnitude of acclimation remains challenging because empirical relationships conflate  
56 the physiological effects of CO<sub>2</sub>, nitrogen limitation, and altered within-plant nitrogen  
57 allocation (Rogers et al., 2017; Smith & Dukes, 2013). We choose here to make a  
58 conservative estimate that maximum photosynthetic rates stay constant as CO<sub>2</sub> increases.

59 This approach is conservative as most estimates predict a decrease in maximum  
60 photosynthetic rates which would enhance the climate impacts of leaf mass per area  
61 acclimation by further reducing the increase in leaf area in response to elevated CO<sub>2</sub>. The  
62 CCLMAPS simulation tested the sensitivity of climate impacts to a simultaneous one  
63 third increase in maximum photosynthetic rates.

64

### 65 ***1.3 Temperature Acclimation of Leaf Mass per Area Estimation and Implementation***

66 We estimated the potential extent of leaf mass per area acclimation to temperature  
67 using biome-specific acclimation relationships from Poorter et al. (2009)'s meta-analysis  
68 of 40 studies and the growing season temperature change due to doubling CO<sub>2</sub> (CC -  
69 CTRL; northern hemisphere JJA and southern hemisphere DJF) at each gridcell. We  
70 estimated the upper bound of leaf mass per area response to temperature by adding the  
71 interquartile range for all plant types reported by Poorter et al. (2009) to the biome-  
72 specific median response (biome-specific interquartile ranges were not reported). The  
73 magnitude of temperature acclimation was not sensitive to interannual variability in CC -  
74 CTRL growing season temperature.

75 We found that temperature could be an influential driver of leaf mass per area  
76 acclimation in boreal and arctic biomes (Fig. S5a). This is because temperature  
77 acclimation occurs when leaves warm from growth-limiting cold temperatures to  
78 temperatures suitable for growth (Poorter et al., 2009). The acclimation response declines  
79 to zero when warming begins from temperatures closer to those suitable for growth  
80 (Poorter et al., 2009). Growing season temperatures below this threshold occur primarily  
81 in boreal and arctic biomes in our simulation. Using a threshold of at least 10% response  
82 we found that four plant functional types - boreal needleleaf evergreen and deciduous  
83 trees, boreal deciduous shrubs, and C<sub>3</sub> arctic grasses - cover 90% of the vegetated area  
84 that we estimate could be impacted by leaf mass per area acclimation to temperature (Fig.  
85 S5b).

86 To test the climate influence of temperature acclimation on our results, we use an  
87 experiment (TCCLMA) that includes a conservative estimate of the upper bound of leaf  
88 mass per area acclimation to both temperature and CO<sub>2</sub>. The TCCLMA simulation is  
89 identical to CCLMA (2xCO<sub>2</sub>; +1/3 leaf mass per area in C<sub>3</sub> plants) except that leaf mass  
90 per area of four plant functional types - boreal needleleaf evergreen and deciduous trees,  
91 boreal deciduous shrubs, and C<sub>3</sub> arctic grasses - were held at control (CTRL) levels. The  
92 corresponding average response of leaf mass per area acclimation to temperature alone  
93 was -15% for gridcells with temperature acclimation. Combining the acclimation of leaf  
94 mass per area to CO<sub>2</sub> (+33%) with the decrease due to temperature acclimation (average  
95 value -15%) results in an average overall increase of +13%. We therefore conservatively  
96 left leaf mass per area values at control levels for these four plant types, representing an  
97 implied 25% decrease in leaf mass per area due to temperature.

98 This approach included a number of assumptions but offered the best estimate of  
99 leaf mass per area temperature acclimation influences on climate and carbon cycling  
100 given the options. It assumes that the temperature acclimation relationship reported by  
101 Poorter et al. (2009) holds at temperatures below 7°C, despite lack of data below this  
102 point; that as shown by Poorter et al. (2009, Fig. 5j) there is no response above 18°C;  
103 and, based on the underlying mechanisms of temperature limiting leaf expansion and sink  
104 growth (Poorter et al., 2009), that growing season rather than annual mean temperature is  
105 the driver. It also assumes that temperature and CO<sub>2</sub> acclimation are additive (no  
106 interaction effect).

107

#### 108 ***1.4 Statistical Analysis***

109 Several variables had time series that were non-normally distributed and  
110 temporally autocorrelated. We therefore used stationary bootstrap methods (Politis &  
111 Romano, 1994; Quilis, 2015) with n = 50,000 to test for differences. The optimal block  
112 length for each stationary bootstrap was determined by automatic estimation (Patton,  
113 2007; Patton et al., 2009; Politis & White, 2004). Time series that failed the Augmented  
114 Dickey-Fuller test for stationarity (Said & Dickey, 1984 and Matlab version 2015b  
115 adftest function) were de-trended prior to bootstrap analysis. Differences were considered  
116 significant at the 95% level using the percentile method (Efron & Gong, 1983; Efron &  
117 Tibshirani, 1994). Confidence intervals for average annual means and differences were  
118 constructed from their bootstrap distributions. T-test and Non-parametric Analysis of  
119 Variance (Zhou & Wong, 2011 modified to use stationary bootstrap) analyses support the  
120 reported findings and conclusions.

121 We tested for spatial relationships between variables at the gridcell scale using  
122 simple, multiple, and stepwise linear regression methods on annual mean values  
123 (CCLMA - CC). Only continental land gridcells (no ocean or coast) that were a least 40%  
124 vegetated were included in the regression analysis. Results were not sensitive to the  
125 selected percentage vegetation. Relationships were considered significant at the 95%  
126 level.

127

128

### 129 **Text S2. Results**

#### 130 ***2.1 Temperature Acclimation of Leaf Mass per Area***

131 Observations of leaf acclimation show that warming temperatures and rising CO<sub>2</sub>  
132 levels have opposing influences on leaf mass per area. As such, warming temperatures  
133 could be hypothesized to offset the influence of CO<sub>2</sub> on leaf mass per area and the  
134 resulting climate and carbon cycling impacts. However, temperature acclimation of leaf  
135 mass per area only occurs at low temperatures (Poorter et al., 2009) and is therefore  
136 limited to boreal and arctic regions.



137 We quantified the influence of temperature acclimation on our CO<sub>2</sub> acclimation  
138 results using a simulation that represents the potential extent of leaf mass per area  
139 acclimation to both temperature and CO<sub>2</sub> (TCCLMA). Specifically, we compared the  
140 differences in the change from the climate change control between two leaf mass per area  
141 acclimation cases: leaf mass per area acclimation to CO<sub>2</sub> alone (CCLMA - CC) and leaf  
142 mass per area acclimation to both CO<sub>2</sub> and temperature (TCCLMA - CC).

143 We found that temperature acclimation of leaf mass per area did not significantly  
144 alter the additional warming beyond the climate change control induced by CO<sub>2</sub>  
145 acclimation of leaf mass per area. Physical warming was unaltered at the global and  
146 latitude band scales (TCCLMA - CC  $\approx$  CCLMA - CC) because temperature acclimation  
147 of leaf mass per area did not significantly offset changes in evapotranspiration and solar  
148 radiation absorbed at the surface, despite slightly compensating for changes in leaf area  
149 index (Fig. S1). Furthermore, temperature acclimation offset only a small portion  
150 ( $\sim$ 1PgC/yr) of the net primary productivity change induced by CO<sub>2</sub> acclimation  
151 (TCCLMA - CC; -5.0 PgC/yr, CI<sub>95%</sub> -4.7 to -5.3). Thus, our estimate of additional  
152 biogeochemical warming due to leaf mass per area acclimation was also similar (+0.1 to  
153 +0.9°C over 100 years for TCCLMA - CC compared to +0.1 to +1.0°C over 100 years  
154 for CCLMA - CC).

155

## 156 ***2.2 Historical Climate Sensitivity to Leaf Mass per Area Change***

157 We found that the influence of historical leaf mass per area acclimation on  
158 climate is likely to be small. From the relationship reported by Poorter et al. (2009), we  
159 estimated that the largest potential extent of historical leaf mass per area change  
160 compared to the pre-industrial period (from 280ppm CO<sub>2</sub> to 355ppm) is +8%. We tested  
161 a much larger one third increase in leaf mass per area for historical simulations at the  
162 control CO<sub>2</sub> concentration of 355ppm (LMA: 1xCO<sub>2</sub>, +1/3 leaf mass per area). This  
163 experiment showed that a stronger than expected increase in leaf mass per area did not  
164 significantly alter historical temperature over land (LMA - CTRL; -0.1°C over land,  
165 CI<sub>95%</sub> 0 to -0.2; -0.2°C globally, CI<sub>95%</sub> -0.1 to -0.2).

166 The effect of leaf mass per area change in the historical period is limited for two  
167 reasons. First, the decrease in leaf area in response to a one third increase in leaf mass per  
168 area was smaller at historical CO<sub>2</sub> (LMA - CTRL: -0.67 m<sup>2</sup>/m<sup>2</sup>, CI<sub>95%</sub> -0.65 to 0.69) than  
169 at future CO<sub>2</sub> (CCLMA - CTRL). This smaller change in leaf area when beginning from  
170 low initial leaf area is consistent with our findings under future CO<sub>2</sub> conditions (see  
171 Results, Fig. S2). The small change in leaf area at historical CO<sub>2</sub> levels muted the  
172 decrease in evapotranspiration (LMA - CTRL: -0.6 W/m<sup>2</sup>, CI<sub>95%</sub> -0.4 to -0.8) compared  
173 to the change at future CO<sub>2</sub> levels (CCLMA - CC). Second, the change in solar radiation  
174 absorbed at the surface was reduced in the historical simulations (LMA - CTRL; -0.3  
175 W/m<sup>2</sup>, CI<sub>95%</sub> -0.1 to -0.6) compared to future simulations (CCLMA - CC), as reduced leaf  
176 area increased albedo (as measured by a change in clear-sky shortwave radiation

177 absorbed at the surface of  $-0.2 \text{ W/m}^2$ ,  $\text{CI}_{95\%}$   $-0.1$  to  $-0.4$ ). Overall, the small decrease in  
178 solar radiation absorbed at the surface and small increase in evapotranspiration resulted in  
179 a near zero change in temperature.

180 Historical net primary productivity was significantly decreased in response to the  
181 one third leaf mass per area increase ( $-6.9 \text{ PgC/yr}$ ,  $\text{CI}_{95\%}$   $-6.6$  to  $-7.2$ ). However, this  
182 value likely overestimates the decrease in productivity by a factor of four, as the  
183 predicted 8% increase in leaf mass per area for historical climate change is approximately  
184 one fourth of the experimental change of 33%. We therefore suggest that  $-2 \text{ PgC/yr}$  is a  
185 more reasonable ballpark estimate for the sensitivity of simulated productivity to leaf  
186 mass per area change at historical  $\text{CO}_2$ . We also note that while the LMA experiment  
187 ( $355 \text{ ppm CO}_2$ ,  $+1/3$  leaf mass per area) is useful for testing the model sensitivity to  
188 changes in leaf mass per area at a historical  $\text{CO}_2$  concentration, we do not expect leaf  
189 mass per area to differ from the control values at  $355 \text{ ppm}$  because these values are based  
190 on observations of leaf mass per area during the present day (White et al., 2000).

191

### 192 ***2.3 Acclimation Altered Balance between Biogeophysical and Biogeochemical*** 193 ***Warming***

194 Leaf mass per area represents the conversion factor between carbon available for  
195 leaf growth and leaf area. Thus increasing leaf mass per area in response to rising  $\text{CO}_2$   
196 alters the balance between biogeophysical and biogeochemical warming by altering the  
197 total leaf area displayed for a given amount of productivity. Plants could overcome this  
198 reduced leaf area by increasing maximum photosynthetic rates. We quantified the  
199 approximate increase in maximum photosynthetic rates and productivity required to  
200 offset the biogeophysical warming induced by leaf acclimation to  $\text{CO}_2$  using a simulation  
201 that simultaneously increased area-based maximum photosynthetic rates ( $V_{\text{cmax}25}$ ,  $J_{\text{max}25}$ ,  
202  $T_{\text{p}25}$ ) and leaf mass per area by one-third (CCLMAPS) compared to the control climate  
203 change simulation (CC).

204 The greater photosynthetic capacity increased global net primary productivity by  
205  $+9 \text{ PgC/yr}$  ( $\text{CI}_{95\%}$  8 to 9) compared to the control climate change simulation (CCLMAPS  
206 - CC) and  $+14 \text{ PgC/yr}$  ( $\text{CI}_{95\%}$  14 to 15) compared to the leaf acclimation simulation  
207 (CCLMAPS - CCLMA). This large increase in productivity mitigated approximately half  
208 of the decline in global leaf area index incurred due to leaf mass per area acclimation  
209 (leaf area index decreased by  $-14\%$  in CCLMAPS - CC compared to  $-26\%$  in CCLMA -  
210 CC). While leaf area decline was not fully compensated for by increasing photosynthetic  
211 rates, total evapotranspiration was no longer significantly reduced compared to the  
212 control climate change simulation (CCLMAPS - CC). Transpiration remained unchanged  
213 and decreased evaporation from leaf surfaces (CCLMAPS - CC;  $-0.4 \text{ W/m}^2$ ,  $\text{CI}_{95\%}$   $-0.4$  to  
214  $-0.5$ ) was compensated for by an increase in evaporation from the soil ( $+0.4 \text{ W/m}^2$ ,  $\text{CI}_{95\%}$   
215  $+0.2$  to  $+0.5$ ). The albedo of the land surface increased slightly globally ( $-0.3 \text{ W/m}^2$ ,  
216  $\text{CI}_{95\%}$   $-0.1$  to  $-0.4$ ) compared to the climate change control consistent with the change in

217 leaf area but did not significantly alter the amount of solar radiation absorbed at the  
218 surface ( $-0.2 \text{ W/m}^2$ ,  $\text{CI}_{95\%}$   $-0.6$  to  $+0.1$ ). As a result, the biogeophysical warming of the  
219 land surface due to a one third increase in leaf mass per area (CCLMA - CC) was  
220 mitigated by a proportional increase in maximum photosynthetic rates (CCLMAPS - CC;  
221  $-0.1^\circ\text{C}$ ,  $\text{CI}_{95\%}$   $0$  to  $-0.2$ );). Thus, a large increase in productivity above that estimated in  
222 our control climate change simulation offset the biogeophysical warming due to leaf  
223 acclimation. However, leaf mass per area acclimation altered the balance between  
224 productivity and biogeophysical land surface processes.

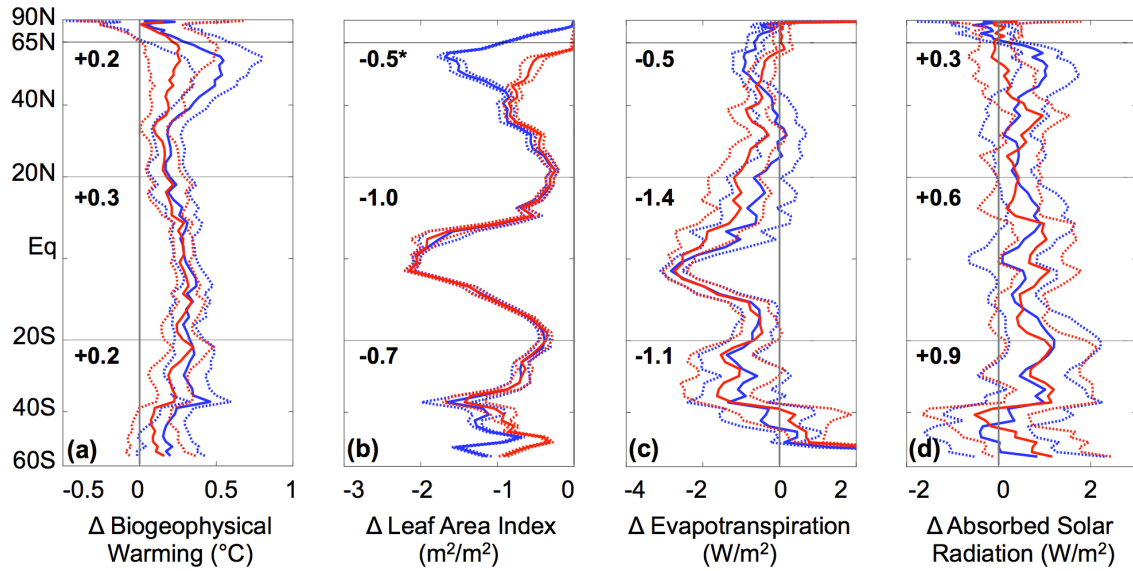


**Figure S1.** Zonal annual mean change over land due to leaf mass per area acclimation to temperature and CO<sub>2</sub> (red, TCCLMA - CC) and leaf mass per area acclimation to CO<sub>2</sub> alone (blue, CCLMA - CC) of (a) biogeophysical warming (°C); (b) leaf area index (m<sup>2</sup>/m<sup>2</sup>); (c) evapotranspiration (W/m<sup>2</sup>); and (d) net solar radiation absorbed at the surface (W/m<sup>2</sup>). Mean differences are shown as solid lines, along with the 95% bootstrap confidence interval (dashed lines). Average zonal mean change on land due to leaf acclimation to temperature and CO<sub>2</sub> (bold numbers) for each latitude band (bounded by dashed lines). Latitude band differences between (CCLMA - CC) and (TCCLMA - CC) significant at the 95% level indicated with asterisk (\*).

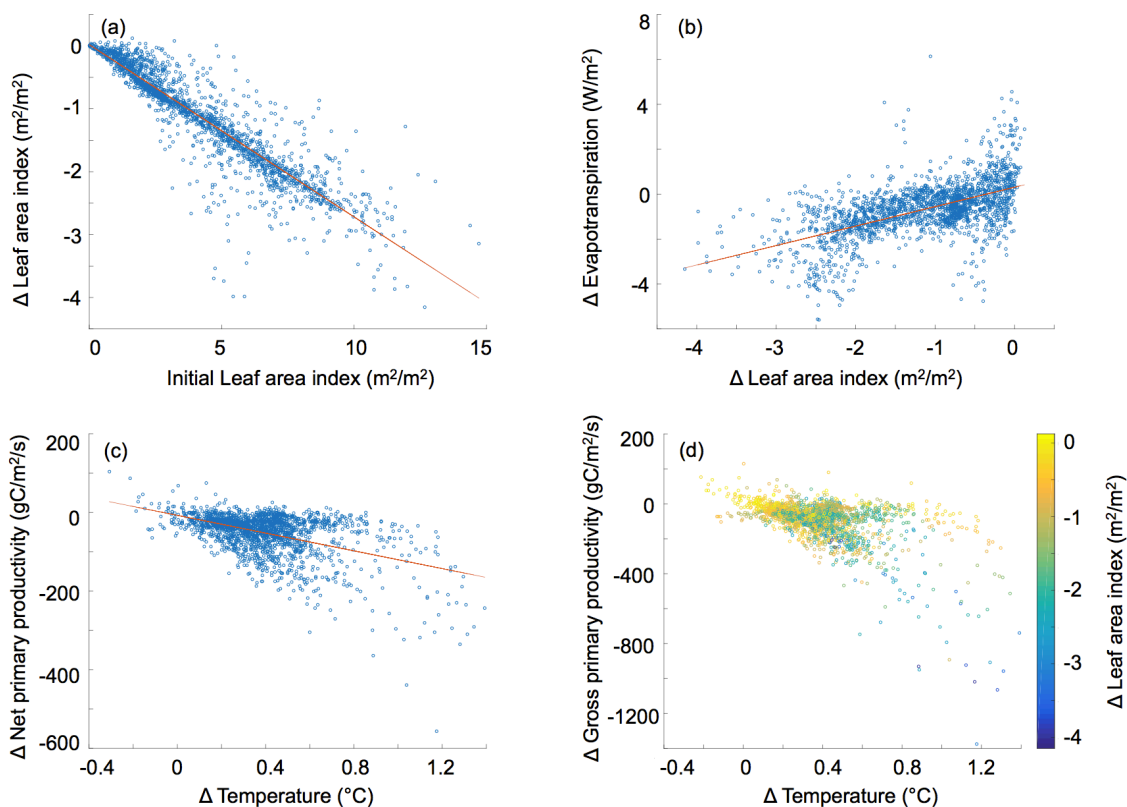


**Figure S2.** Scatterplots between gridcell level (a) initial leaf area index (CC) and the change in leaf area in response to leaf acclimation to  $\text{CO}_2$  ( $R^2 = 0.83$ ); (b) the changes in leaf area and evapotranspiration ( $R^2 = 0.32$ ); (c) the changes in temperature and net primary productivity ( $R^2 = 0.24$ ); and (d) the changes temperature, leaf area index, and gross primary productivity (multiple regression  $R^2 = 0.32$ ). Ordinary least squares regression lines plotted in red (a-c).

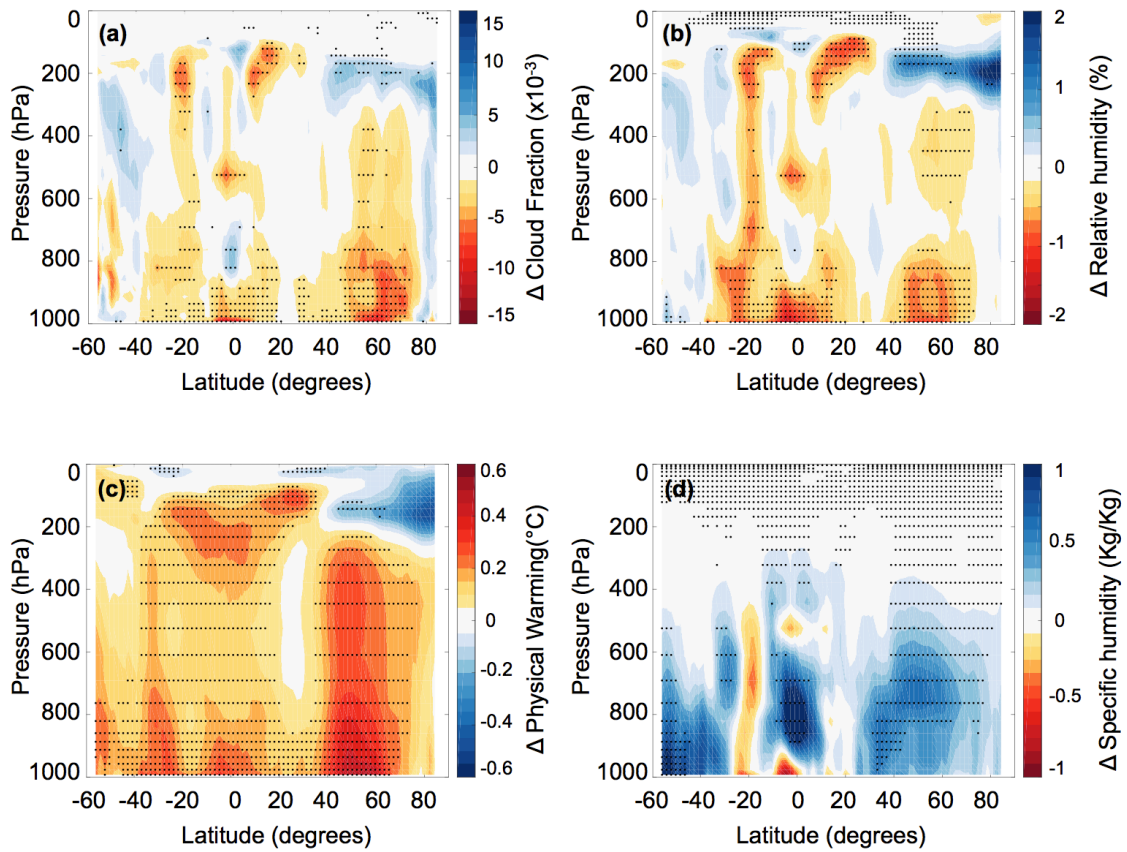


**Figure S3.** Zonal annual mean change over land due to leaf acclimation of (a) cloud fraction; (b) relative humidity(%); (c) biogeophysical warming ( $^{\circ}\text{C}$ ); and (d) specific humidity (Kg Water/Kg). Stippling indicates significance at the 95% level.

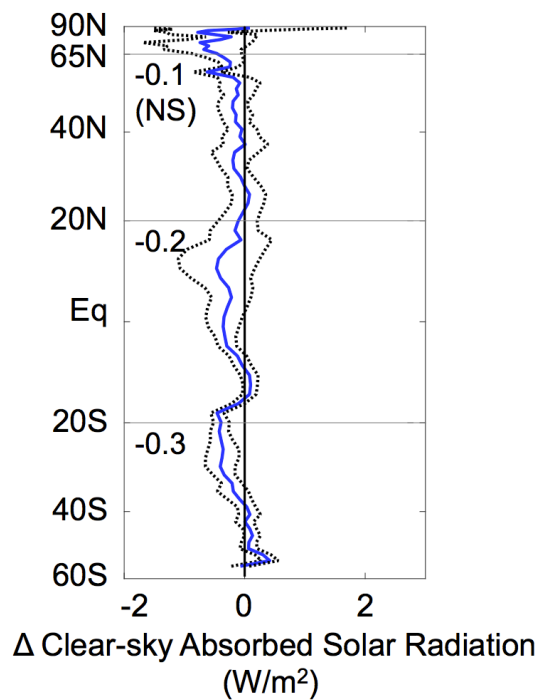


**Figure S4.** Zonal annual mean change over land due to leaf acclimation (CCLMA - CC) of clear-sky solar radiation absorbed at the surface ( $\text{W/m}^2$ ). The mean difference is shown in blue, along with the 95% bootstrap confidence interval (dashed black) and average zonal mean change on land (bold numbers) for each latitude band (bounded by dashed lines).

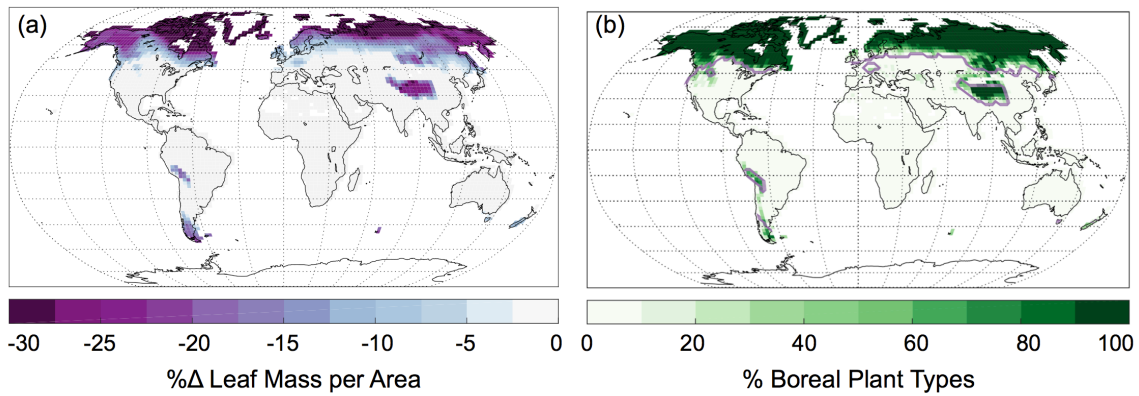


**Figure S5.** (a) Potential extent of leaf mass per area change (%) due temperature acclimation estimated from growing season temperature change (CC - CTRL) and biome-specific acclimation relationships from Poorter et al. (2009). (b) Percent of simulated vegetated area covered by boreal plant types (boreal needleleaf evergreen and deciduous trees, boreal deciduous shrubs, and C<sub>3</sub> arctic grasses). Purple contours indicate -5% threshold for change in leaf mass per area due to temperature acclimation.



**Table S1** List of Earth System Model Simulations

Name	[CO <sub>2</sub> ]	Δ LMA	Δ PS Rates	Description
CTRL	1xCO <sub>2</sub>	-	-	<i>control</i>
LMA	1xCO <sub>2</sub>	+1/3	-	<i>historical climate + leaf mass per area change</i>
CC	2xCO <sub>2</sub>	-	-	<i>climate change only</i>
CCLMA	2xCO <sub>2</sub>	+1/3	-	<i>climate change + upper range of leaf mass per area acclimation to CO<sub>2</sub></i>
CCLMAPS	2xCO <sub>2</sub>	+1/3	+1/3	<i>climate change + upper range of leaf mass per area acclimation to CO<sub>2</sub> + greater photosynthetic rates</i>
TCCLMA	2xCO	+1/3, no Δ boreal & arctic	-	<i>climate change + upper range of leaf mass per area acclimation to CO<sub>2</sub> and temperature</i>

Note: [CO<sub>2</sub>], prescribed atmospheric CO<sub>2</sub> concentration (1xCO<sub>2</sub> = 355ppm, 2xCO<sub>2</sub> = 710ppm); ΔLMA, prescribed change in leaf mass per area for C<sub>3</sub> plants; ΔPS Rates, prescribed change in maximum photosynthetic rates per area for C<sub>3</sub> plants.

**Table S2** Confidence intervals for annual mean changes over land due to leaf trait acclimation (CCLMA - CC).

	Global		S. Extratropics		Tropics		N. Extratropics		N. High Latitudes	
	Mean	(95%CI)	Mean	(95%CI)	Mean	(95%CI)	Mean	(95%CI)	Mean	(95%CI)
Biogeophysical Warming (°C)	0.3	(0.2, 0.4)	0.3	(0.2, 0.4)	0.3	(0.2, 0.4)	0.4	(0.2, 0.5)	0.2	(0.0, 0.5)
Net primary productivity (PgC/yr)	-5.8	(-5.5, -6.0)	-0.8	(-0.7, -1.0)	-2.5	(-2.3, -2.8)	-2.1	(-1.9, -2.3)	-0.3	(-0.2, -0.3)
Leaf area index (m <sup>2</sup> /m <sup>2</sup> )	-0.9	(-0.9, -1.0)	-0.8	(-0.7, -0.8)	-1.0	(-1.0, -1.1)	-1.0	(-0.9, -1.0)	-0.6	(-0.5, -0.6)
Evapotranspiration (W/m <sup>2</sup> )	-0.7	(-0.5, -0.9)	-0.9	(-0.2, -1.6)	-1.2	(-0.8, -1.5)	-0.4	(-0.1, -0.6)	-0.5	(-0.3, -0.7)
Transpiration (W/m <sup>2</sup> )	-1.4	(-1.2, -1.5)	-1.9	(-1.4, -2.4)	-1.7	(-1.5, -1.9)	-1.1	(-1.0, -1.3)	-0.6	(-0.4, -0.7)
Leaf Evaporation (W/m <sup>2</sup> )	-0.8	(-0.7, -0.8)	-0.7	(-0.5, -0.8)	-1.3	(-1.2, -1.5)	-0.5	(-0.5, -0.6)	-0.3	(-0.3, -0.4)
Soil Evaporation (W/m <sup>2</sup> )	1.4	(1.3, 1.6)	1.6	(1.3, 1.9)	1.9	(1.8, 2.1)	1.3	(1.1, 1.4)	0.4	(0.3, 0.5)
Absorbed Solar Radiation (W/m <sup>2</sup> )	0.6	(0.3, 0.8)	0.8	(0.1, 1.5)	0.6	(0.3, 1.0)	0.6	(0.3, 0.9)	-0.1	(-0.4, 0.2)